(NASA-CR-189433) CEPHEID TEMPERATURE AND THE BLAZHKO EFFECT (Computer Sciences Corp.) 52 p

N95-31819

Unclas

G3/90 0058473

Final Report for Contract NAS-31845
Short Title of Project: Cepheid/Blazhko Effect
Task 5779
Principal Investigator: Terry Teays

Two separate research projects were covered under this contract. The first project was to study the temperatures of Cepheid variable stars, while the second was a study of the Blazhko effect in RR Lyrae, both of them using IUE data. They will be reported on separately, in what follows.

Cepheid Temperatures

The purpose of this project was to establish the temperatures of Cepheid variable stars by fitting their energy distributions to model atmospheres. Published photometry from the literature was used to provide the fluxes in both the infrared (IR) and visual parts of the spectrum, These were combined with the available IUE archival data for δ Cephei. Since there were crucial pulsation phases missing in the archival data, new observations were obtained under this program. All of the spectra were obtained and have been reduced. The comparison with model atmospheres required that we have additional ones calculated, to fit the specific requirements of the stars under study. Dr. John Lester kindly calculated the specific models needed, using the latest version of the Kurucz stellar atmospheres code for use in this study.

The comparison of these data with model atmospheres to make precise temperature determinations required a number of preliminary studies to verify that our techniques were correct and sufficiently precise for this study. The first test was to study a Cepheid with a Main Sequence companion, using IUE spectra. We examined the well studied star S Muscae, and determined its temperature and other parameters, based on its known orbit. This work has been published (1), and a copy is attached. The second test was to examine a non-variable F supergiant, which is as close to a Cepheid in structure as possible, yet without the added complexity of pulsation. For this test we chose α Persei, which is a member of a well-studied cluster, and therefore has well-determined observational parameters. This study was successful, and proved the validity of our approach. This result has been presented this past February at the Cape Town pulsation meeting on *Astrophysical Applications of Stellar Pulsation.* A copy of the short description of the poster paper which will appear in the published proceedings (2) is attached. A full description of this work has been prepared and is being submitted to AJ. A preprint of this submission is attached (3).

The final results of the applications to the Cepheids are in preparation. We have completed all of the necessary analyses and comparisons with model atmospheres for the δ Cephei data, and determined the temperatures at all phases. A final paper on this work will be submitted (probably to AJ) soon. (Publication charges will be paid for by the Lead Investigator for that final paper.) We have presented the results in a poster paper at the Tucson AAS meeting in 1995 January and at the Cape Town pulsation conference.. A copy of the abstract (4), which appeared in BAAS, is attached (the abstract for the Cape Town meeting was identical).

Blazhko Effect

The purpose of this program was to study the Blazhko effect in RR Lyrae type stars. I conducted a multi-wavelength, multi-site campaign to follow RR Lyr (the brightest star of this type, and one which shows the Blazhko effect) through a complete pulsation cycle, at a variety of Blazhko phases. One of my collaborators and I acquired and reduced all of the IUE data. We have constructed visual (FES) and ultraviolet light curves from these data and performed Fourier decomposition analysis on all of them,

which has produced some very interesting results, which have spurred new observations and theoretical models. These results have been compared with non-Blazhko RR Lyrae stars. The visual and ultraviolet amplitudes have also been compared to the one-zone models of Antonelo, producing surprisingly good (perhaps somewhat fortuitously so) agreement.

The first results of this campaign were presented at the pulsation conference in Victoria, Canada (IAU Colloquium 139, *New Perspectives on Stellar Pulsation and Pulsating Variable Stars*), where I gave an invited review talk on this subject. A copy of the published conference proceedings paper is attached (5). A more quantitative poster paper was presented at the 27th ESLAB Conference on *Frontiers of Space and Ground-Based Astronomy.* A copy of the published version of the poster is attached (6). Finally, I gave a review talk on the Blazhko effect for CSC's Center for Scientific Research colloquium series.

REFERENCES

(1) Evans, N. R., Massa, D., & Teays, T. J. 1994, AJ, 108, 2251
(2) Evans, N. R., Teays, T. J., Taylor, L. T., Lester, J. B., & Hindsley, R. B. 1995, in Astrophysical Applications of Stellar Pulsation, ed. R. Stobie & P. Whitelock, (San Francisco: ASP), in press
(3) Evans, N. R., Teays, T. J., Taylor, L. T., Lester, J. B., & Hindsley, R. B. 1995, being submitted to AJ
(4) Evans, N. R. & Teays, T. J. 1995, BAAS, 27, 760
(5) Teays, T. J. 1993, in New Perspectives in Stellar Pulsation and Pulsating Variable Stars, ed. J. M. Nemec & J. M. Matthews, (Cambridge: Cambridge Univ. Press), 410
(6) Teays, T. J., Bonnell, J. T., Schmidt, E. G., Guinan, E. F., & Barnes, T. G. III, 1994, in Frontiers of Space and Ground-Based Astronomy, ed. W. Wamsteker, Y. Kondo, & M. S. Longair, (Dordrecht: Kluwer), 597

Terry Teays

THE ASTRONOMICAL JOURNAL VOLUME 108, NUMBER 6 DECEMBER 1994

S MUS B REVISITED[1]

NANCY REMAGE EVANS

Space Astrophysics Lab., Institute for Space and Terrestrial Sciences, York University, 4700 Keele St., North York, Ontario M3J 1P3, Canada
Electronic mail: evans@nereid.sal.ists.ca

DERCK MASSA

Applied Research Corporation, 8201 Corporate Dr., Landover, Maryland 20785
Electronic mail: massa@iue.gsfc.nasa.gov

TERRY J. TEAYS[2]

Computer Sciences Corp., Science Programs, 10000 A Aerospace Rd., Lanham-Seabrook, Maryland 20706
Electronic mail: teays@iuegtc.gsfc.nasa.gov

Received 1994 March 1; revised 1994 August 10

ABSTRACT

IUE high dispersion spectra have been used to investigate the spectral type of the companion of the classical Cepheid S Mus, using Si II and III lines near 1300 Å. In addition, the energy distribution from 1200 to 3200 Å from *IUE* low resolution spectra has also been compared with standard stars. The resulting spectral type is B3.5 V [with a reddening of $E(B-V)=0.21$ mag]. Using the magnitude difference between the two stars and the Cepheid luminosity, the binary components are compared with evolutionary tracks computed by four groups. A mass between 5.5 and 6.0 $M_\odot$ results from all tracks. On the other hand, the relatively small luminosity difference between the two stars is only consistent with tracks with minimal convective overshoot and a companion nearing the end of the main sequence phase.

1. INTRODUCTION

S Mus is a classical Cepheid and a member of a binary system, which makes it a candidate for mass determination. The mass of the Cepheid can be obtained from an orbital velocity ratio for the two stars from ground-based and ultraviolet measurements, and a mass for the companion from its spectral type. Progress toward this goal is promising. An orbit has been derived (Lloyd Evans 1982; Evans 1990). Furthermore, because the companion, S Mus B, is both hot and bright, high resolution spectra have been obtained with the International Ultraviolet Explorer Satellite (*IUE*) in both the short (1200 to 2000 Å) and long (2000 to 3200 Å) wavelength regions. Velocity measurements from these spectra have been investigated (Böhm-Vitense *et al.* 1990 hereafter referred to as BCCW; Böhm-Vitense 1986). Because of the size of the *IUE* spectrograph aperture, the positioning of the star causes an uncertainty in the absolute accuracy of a velocity of typically 5 km s^{-1}. For this reason, the long wavelength spectra are more useful that the short wavelength spectra, since both stars make a contribution to the flux in the long wavelength region. The ground-based orbital and pulsation velocities can be combined with the velocity difference for the two stars measured from the *IUE* long wavelength spectra to determine the absolute orbital velocity of the companion.

Unfortunately, although both stars contribute a significant amount of flux in the long wavelength region (see Fig. 5 below), the velocity of the companion is not easy to measure because the mid B star has few strong lines in the wavelength region 2200 to 2700 Å, where it dominates the spectrum. Since the G supergiant spectrum of the Cepheid has numerous strong lines, it dominates the cross-correlation velocity measures, unless it makes only a very small contribution to the composite spectrum. Furthermore, the few strong resonance lines in this region are probably contaminated by interstellar absorption (Rodrigues & Böhm-Vitense 1992). The difficulties in determining the velocity of S Mus B from the *IUE* spectra are illustrated by Fig. 4(b) in BCCW, which shows the cross correlation function and Table VII in the same study showing the spread of velocities within a single spectrum.

In order to determine the Cepheid mass from the orbital velocity ratio, the mass of the companion must be known. It is the purpose of this paper to investigate the spectral type, temperature, and mass of the companion further. These parameters have been investigated several times previously. Böhm-Vitense & Proffitt (1985) derived a temperature of 17 700 K from the *IUE* energy distribution. BCCW determined a spectral type by comparing the *IUE* spectra of B stars with that of S Mus B. In addition, they compared the equivalent widths of spectral features at 1400, 1300, 1261 Å, and Lyman α from *IUE low resolution* spectra with those of standard stars. They concluded that the companion has a spectral type of B5 V. A temperature or spectral type determined from the energy distribution depends heavily on the dereddening. This is particularly true for stars with spectral types hotter than mid B. For cooler stars, the peak of the energy distribution occurs in the SWP wavelength region

[1] *IUE* Archival Research.
[2] Staff Member of the International Ultraviolet Explorer Observatory.

0004-6256/94/108(6)/2251/8/$0.90

TABLE 1. *IUE* high dispersion spectra for comparison with S Mus.

Star	HD	Spectral type	Image	$V \sin i$ (km s^{-1})
γ Ori	HD 35468	B2 III	SWP 8026	60
2 Ori	HD 35039	B2 IV–V	SWP 3580	13
8 Peg	HD 209008	B3 III	SWP 20593	75
ι Her	HD 160762	B3 IV	SWP 29818	10
40 Tau	HD 25558	B3 V	SWP 20595	40
τ Ori	HD 34503	B5 III	SWP 3825	45
τ Her	HD 147394	B5 IV	SWP 3246	27
			SWP 3245	27
19 Tau	HD 23338	B6 IV	SWP 40508	133
eta Sex	HD 90994	B6 V	SWP 7928	114

TABLE 2. *IUE* high dispersion spectra of S Mus.

Spectrum
SWP 17503
SWP 17496
SWP 22819
SWP 31543
SWP 32685
SWP 32686
SWP 32719

1200 to 2000 Å) and fluxes at wavelengths shorter than the eak are extremely sensitive to the temperature. The energy istribution changes so markedly with small changes in temerature that a small uncertainty in the reddening has an nsignificant effect on the temperature determined. For earier B stars, the energy distribution increases monotonically o shorter wavelengths and an incorrectly dereddened specrum can mimic an incorrect temperature.

Evans (1990, hereafter referred to as Paper I) also discussed the spectral type of the companion, stressing that the eddening of the system derived from the colors of the Cepheid must be determined iteratively since the companion affects the observed colors of the Cepheid. The spectral type of S Mus B resulting from this analysis is also B5 V.

The *IUE* spectra of S Mus are rediscussed here for several reasons. The technique of analysis, in particular the treatment of reddening, has evolved somewhat, as described in Evans (1991). In addition, the previous analysis did not discuss the luminosity difference between the stars. Finally, it has been discovered that small aperture spectra with only partial throughput were used in Fig. 3 of Paper I, so the corrected colors and magnitudes need to be redetermined.

In addition to the low resolution SWP spectra of S Mus, there are a number of high resolution SWP spectra available in the *IUE* archives. Because of the importance of an accurate spectral type or temperature and hence mass for S Mus B, we have investigated the companion using these high resolution spectra also. Specifically, the study of Massa (1989) has discussed the use of silicon lines on *IUE* high resolution spectra to determine spectral types and luminosities in early and middle B stars. We have followed the lines of this analysis for S Mus B.

In the following section, the spectral information from the high resolution spectra and the low resolution spectra will be presented, followed by a discussion of the mass of S Mus B and its evolutionary state.

2. HIGH RESOLUTION SPECTRA

In order to determine the spectral type of S Mus B, we have selected stars from the list studied by Massa with spectral types B2 through B5 and luminosity classes V to III. We have also added B6 V and B6 IV stars to the list. The spectra used are listed in Table 1. (In some cases, additional spectra of these stars have also been investigated.) The stars were originally selected to have low rotation velocities, as shown in Table 1. (Rotational velocities are taken either from Massa or the Bright Star Catalogue.) Table 2 lists spectra of S Mus which have been compared to confirm the reality of the features. SWP 17503 was the spectrum used as the standard for S Mus, and it is the one shown in the figures below. The spectra were processed with standard Regional Data Analysis Facility (RDAF) software as described by Massa. The figures show the spectra smoothed into three point bins.

The best temperature indicator in the relevant spectral range was found by Massa to be the Si II line at 1265 Å, which increases in strength from B2 through B6. The comparison of S Mus with stars in Table 1 is shown in Figure 1. The spectra have been aligned in wavelength; normalization was done by a simple mean of the flux in a 25 Å interval surrounding 1265 Å. The B3 and B5 spectra are the most similar to S Mus B; however, it is clear in Fig. 1 that both the B5 spectra have stronger 1265 Å lines than S Mus B, making B3 the best match.

The region from 1290 to 1315 Å contains a number of strong features, as well as many weaker ones. The comparison between S Mus and stars with a range of spectral types is shown in Fig. 2. Because of the difficulty in choosing regions of real continuum, we have used the overall mean flux for scaling as in Fig. 1. The three lines found by Massa to be the most useful for temperature are Si III 1294, Si III 1299, and Si II 1309. However, the Si III lines show less change between B3 and B5 than for earlier spectral types. As would be expected, the Si III lines decrease in strength and the Si II lines grow as the spectral type becomes later.

Figure 2 shows that B3 and B5 match best with S Mus B. Close inspection, however, shows that the wings of the Si III lines of the B5 stars are narrower than S Mus B stars. Similarly, the Si II line is slightly wider in the B5 stars than S Mus B. In fact, the agreement between S Mus B and the B3 V star is striking, both in the Si III and II lines and in the entire spectral region. The overall agreement in addition to the Si agreement is important, since it indicates similar weak features as well as strong ones. We note, however, that similar comparisons indicate that S Mus B is slightly cooler than the B3 IV star ι Her.

In summary, the Si III and II diagnostics displayed in Figs. 1 and 2 both show that S Mus B has a spectral type closer to B3 than to B5.

We have also produced similar comparisons for 1417 Å, which was found by Massa to be a good luminosity indicator. However, it is most effective in distinguishing supergiants from main sequence stars; stars with luminosity classes V to

FIG. 1.
and sta
line at
fluxes

III ar
in the
1 and
discu
singl
temp
indic
Fi
B ar

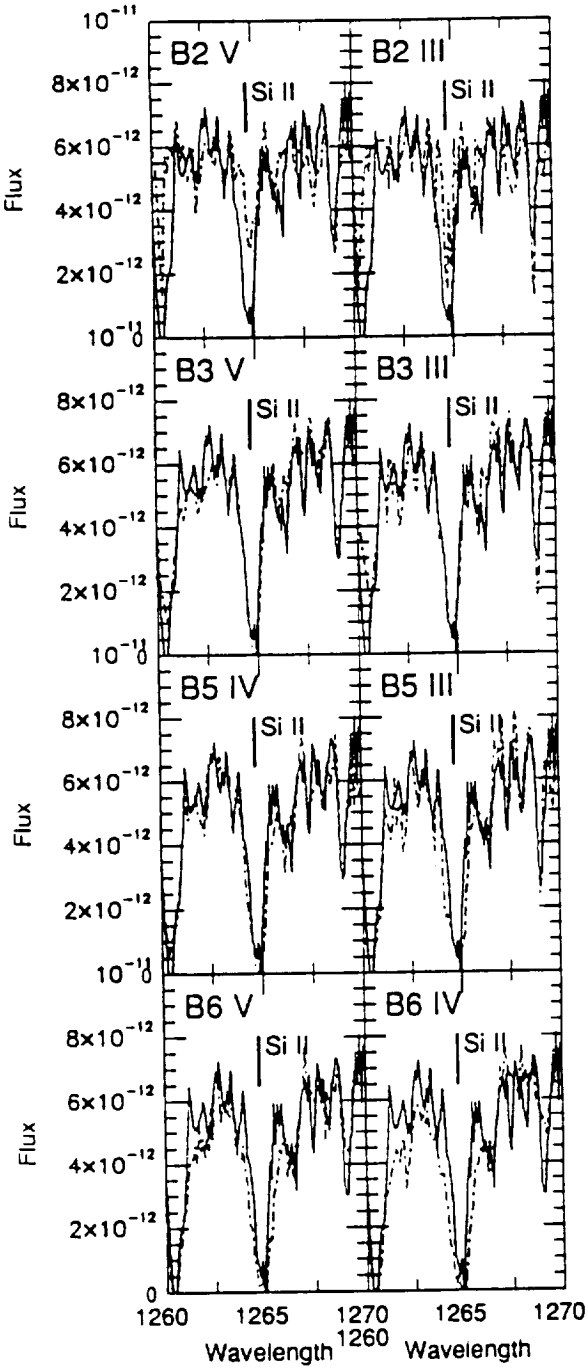

FIG. 1. The comparison between high resolution spectra of S Mus (solid) and stars of a range of spectral types (dot-dashed) in the region of the Si II line at 1265 Å. The spectral type of the standard star is in the upper left. All fluxes in graphs are in erg cm^{-2} s^{-1} Å^{-2}; all wavelengths are in Å.

III are mixed together. We found little additional information in the examination of these plots since all the stars in Tables 1 and 2 are within the main sequence band. Although not discussed explicitly by Massa (1989), 1312.59 Å is a Si III singlet with the same lower level as 1417 Å. It responds to temperature and gravity in the same way as 1417 Å, and indicates that S Mus B is closer to B3 V than B3 III.

Figures 1 and 2 also show that the line profiles of S Mus B are the same width as the low rotation stars. We have explored this in a little more detail. We have convolved the spectrum of S Mus B with a Gaussian with a σ of 50 km s^{-1}, which is a good approximation for rotation $v \sin i = 100$ km s^{-1}. The lines in the convolved spectrum are clearly not as deep as the original spectrum. On the other hand, the lines in S Mus B in Figs. 1 and 2 have the same depth as either the B3 or B5 standard stars. Altogether, the excellent match between S Mus B and the standard stars confirms that S Mus B has a low rotation velocity.

3. LOW RESOLUTION SPECTRA

IUE low resolution spectra can be used to obtain additional information about the spectral type and also to determine the magnitude difference between the two stars in the S Mus system. They were reduced as discussed by Evans (1991) using the SUN version of the RDAF software at the Space Astrophysics Laboratory of the Institute for Space and Terrestrial Science. Spectra were dereddened using a Seaton reddening law. The spectra which were used are listed in Table 3. The phases are computed from the period and epoch given by Szabados (1989). The light and color curves of Stobie (1970) were used.

Since the "continuum" spectrum of S Mus B increases from 2000 to 1200 Å, a change in E($B-V$) changes the slope, and hence the spectral type. Part of the purpose of this study is to evaluate the effect of the companion on the measured colors of the system in the visible, and hence the effect on the photometrically determined reddening. A trial E($B-V$) is selected, a companion spectral type tentatively determined, and then the reddening is reevaluated. Once a reddening has been found consistent with the colors corrected for the companion, however, a small change in spectral type has very little effect on the reddening. The details of the reddening determination are discussed in Evans (1989) and Evans (1991). The process was begun using E($B-V$) $=0.27$ mag from Dean *et al.* (1978). The corrected reddening was determined from their $(B-V)-(V-I)$ (Kron Cousins system) relations.

Figure 3 shows the comparison between S Mus B and the spectral type standards for B3 V and B4 V (17 Vul and HD 64904, the "dagger" spectral standards listed in the *IUE* Spectral Atlas; Wu *et al.* 1983) and also the B3.5 V spectrum interpolated between them. [The adopted value for the reddening for S Mus, E($B-V$) $=0.21$ mag is used. The reddenings for the standard stars are those from the *IUE* Spectral Atlas, and are all small.] The spectra have been scaled to match at 1600 Å. The region from 1170 to 1400 is used to determine the spectral type. Both B3 and B4 standards match reasonably well, but the B3.5 V spectrum has the best match between 1250 and 1350 Å and also the best overall match between 1200 and 1900 Å. One criterion which is not affected by the reddening is the width of the Ly α line. However, there is a reseau in the short wavelength side of the line, so only the long wavelength side should be considered. S Mus B is the most similar to B4 V at Ly α. (Correction for interstellar Ly α absorption using a simple model shows that it has a negligible effect on the wings.) We are, however, puzzled by the fact that the width of Ly α is the most dis-

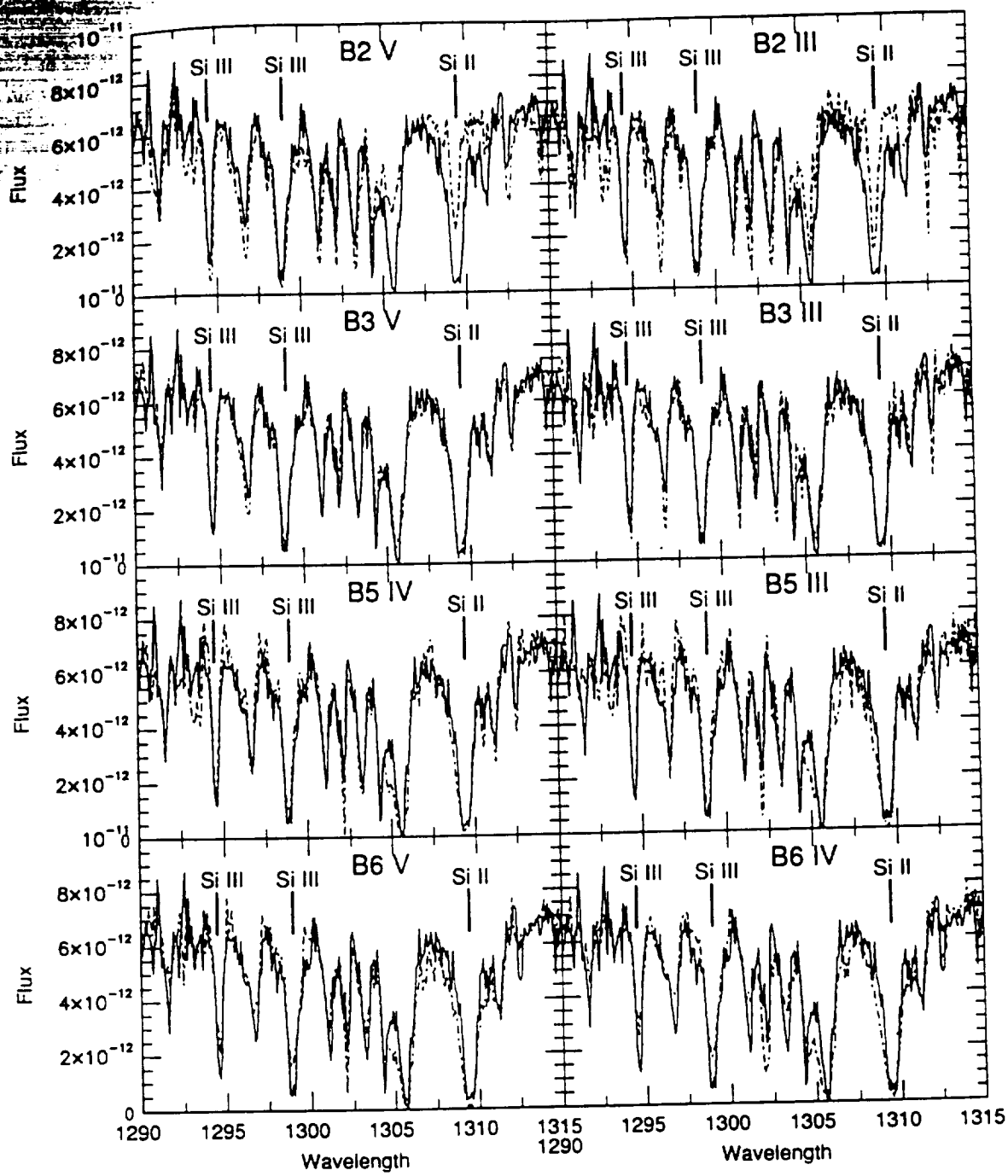

FIG. 2. The comparison between high resolution spectra of S Mus and the stars of a range of spectral types. The symbols are the same as in Fig. 1.

cordant of the criteria discussed here. Figure 4 shows the same comparison for the entire *IUE* wavelength region. Here, B3 V is a closer match, since, for the other two, the comparison star has too much flux longward of 1700 Å. This is even true longward of 2600 Å, since the Cepheid makes a contribution here. The long wavelength spectrum, decomposed to show the contributions of the two stars, is shown in Fig. 5. Here the Cepheid is represented by the spectra of two nonvariable supergiants, interpolated to the same $(B-V)_0$ as the Cepheid (corrected for the light of the companion). Details of the supergiants used are given in Evans *et al.* (1990). The companion is the B3.5 V spectrum, using the scale factors determined from the short wavelength spectrum [Fig. 3(b)]. The contribution of the Cepheid is visible from 2800 to 3200 Å.

TABLE 3. *IUE* low dispersion spectra of S Mus.

Image	JD 2 400 000	Pulsation phase	V (mag)	$B-V$ (mag)	Observer
SWP 19503	45414.917	0.59	6.35	0.96	Reipurth
LWR 15531	45414.923	0.59	6.35	0.96	Reipurth

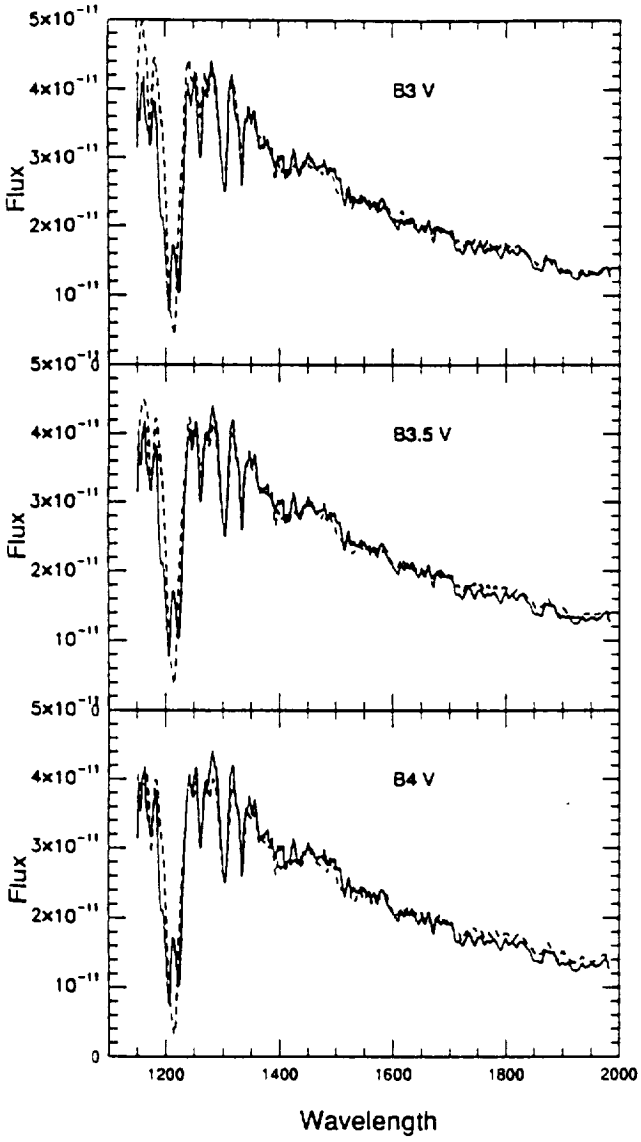

FIG. 3. The comparison between the low resolution spectrum of S Mus B (solid) and spectral standards (dashed). The low resolution spectra of S Mus B have been dereddened; the high resolution spectra in Figs. 1 and 2 have not been dereddened. (a) B3 V spectral standard. (b) B3.5 V spectrum interpolated between the B3 V standard and the B4 V standard. (c) B4 V spectral standard.

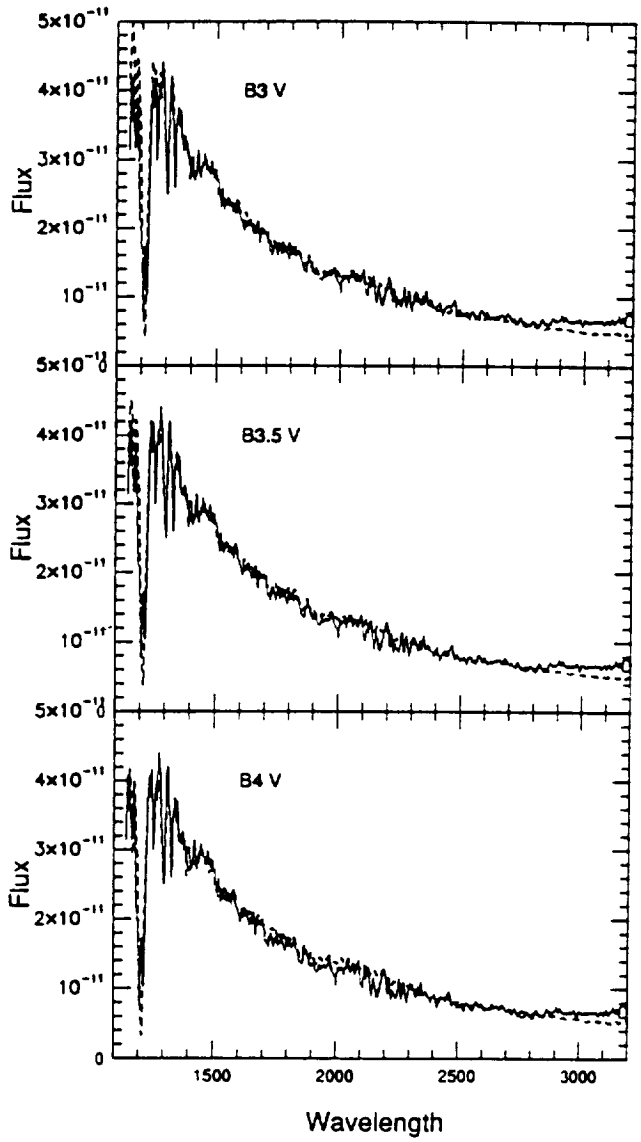

FIG. 4. The same comparisons as in Fig. 3, except that the full *IUE* wavelength range from 1150 to 3200 Å is shown.

From the individual comparisons in Figs. 3 and 4 we can make distinctions of half a spectral subclass. The results from the various approaches are summarized below:

(1) B3 main sequence band (class V to III, between the ZAMS and the TAMS) from high dispersion spectra, but slightly cooler than ι Her (B3 IV).
(2) B3.0 V from the overall flux distribution (Fig. 4).
(3) B3.5 V to B4 V from the details in the spectrum near 1300 Å, including Lyman α (Fig. 3).

From this summary, we adopt B3.5 V as the spectral type for S Mus B. As mentioned above, the corrections to the colors, and hence the final reddening value are not very sensitive to small changes in the spectral type.

As part of the analysis, we have also investigated the effect which the form of the reddening law may have on the

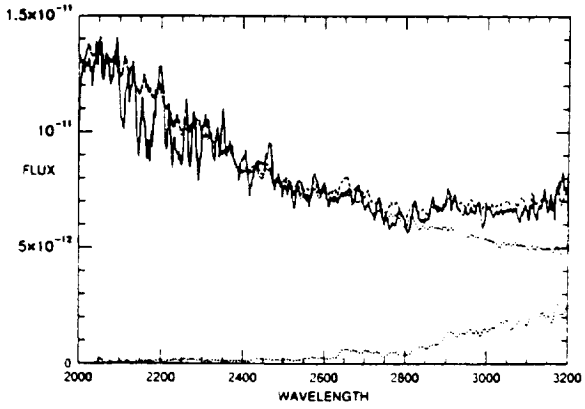

FIG. 5. The spectrum of S Mus decomposed into the two component stars. The observed spectrum is the solid line. The two short dotted lines are standard spectra representing the hot and cool components. The dashed line is the sum of the two components.

TABLE 4. Corrected magnitudes and colors of S Mus.

	V_0 Cep+comp (mag)	$(B-V)_0$ Cep+comp (mag)	V_0 Cep (mag)	$(B-V)_0$ Cep (mag)
Mean	5.41	0.62	5.47	0.69
Phase 0.59	5.62	0.75	5.69	0.86

B3.5 V Companion:
$V_0 = 8.57$ mag
$(B-V)_0 = -0.19$ mag
$E(B-V) = 0.21$ mag

spectral type of the companion. We have also dereddened the spectra of S Mus using the extinction law of Cardelli *et al.* (1989, hereafter referred to as CCM) with $R = 3.2$. This relation is virtually the same as the Seaton (1979) relation used above except that the CCM relation results in larger fluxes for wavelengths shorter than 1500 Å. This suggests an earlier spectral type than B3 V. However, since the high resolution spectra (Figs. 1 and 2) rule out an earlier spectral type, we accept the Seaton dereddening.

Table 4 shows the magnitudes and corrected colors for final $E(B-V) = 0.21$ and B3.5 V companion with $V_0 = 8.57$ and $(B-V)_0 = -0.19$. The color of the B3.5 V companion is taken from Johnson (1966).

Figure 6 shows an additional comparison between spectra and model atmospheres from Kurucz (1991). Models with $\log g = 4.0$ and solar abundance have been used. Clearly, the 16 000 K atmosphere is cooler than S Mus B. For the two hotter atmospheres, there is some disagreement between the models and the spectra in the sense that the models have too little flux from 1400 to 1600 Å. The agreement between the S Mus B spectrum and the B3 V and B4 V standard stars in Fig. 3 indicates that the disagreement in Fig. 6 is not a problem with the S Mus B spectrum. [Since the SWP spectrum was obtained in 1983, it is within two years of the observations of most of the standard stars. This means that flux differences due to camera sensitivity changes should usually be less than 2% as shown by Garhart (1993) and are insignificant]. If the normalization is made from 1600 to 1700 Å, the flux between 1200 and 1600 Å is systematically low. Normalization from 1400 to 1800 Å in Fig. 6, on the other hand, would increase the model flux so that it would be too high from 1600 to 2000 Å. Because of this disagreement and the difficulty with the normalization, there is some uncertainty in the temperature determined from Fig. 6. The Lyman α line is a better match to the 18 000 K model. (The long wavelength side should be compared because the short wavelength side is distorted by a camera reseau mark.) We conclude from Fig. 6 that the spectrum is matched about equally satisfactorily by the 20 000 and 18 000 K models, but that the difference between the models and spectra precludes a more detailed temperature determination.

4. DISCUSSION

Having established the spectral type of S Mus B, the next step is to investigate its luminosity. To do this, we take the approach of Evans (1994), to use the absolute magnitude for

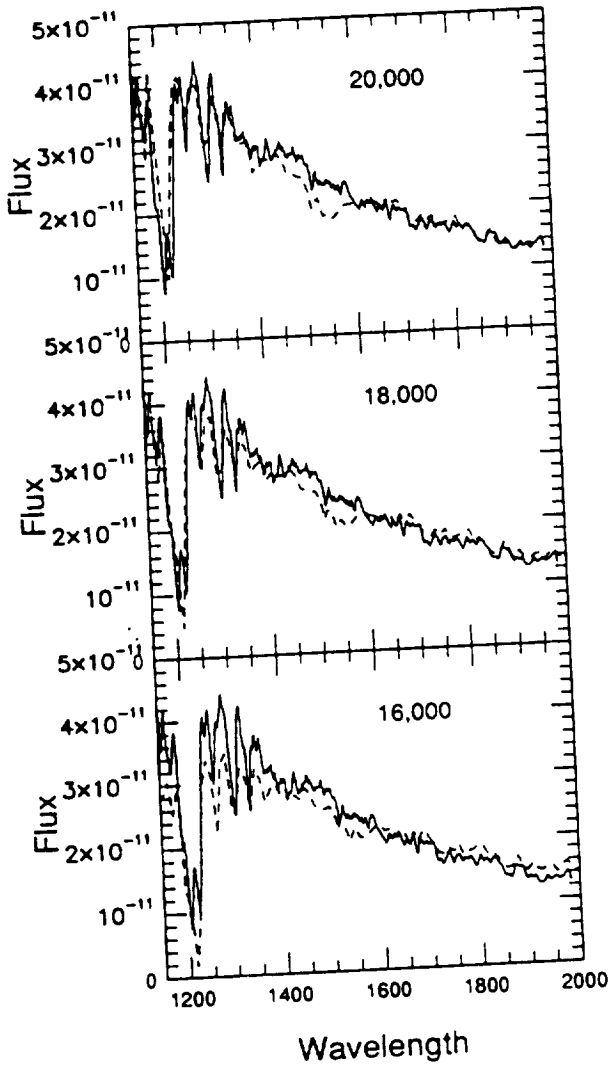

FIG. 6. S Mus B (solid) compared with Kurucz model atmospheres for three temperatures (dashed). The temperatures in K are indicated in the upper right. All atmospheres are for $\log g = 4.0$ and solar abundance.

the Cepheid from the period–luminosity–color relation (PLC) and the magnitude difference between the two stars to determine the luminosity of the companion. From the period–luminosity–color (PLC) relation of Feast & Walker (1987), the absolute magnitude of the Cepheid is −4.14 mag. The magnitude difference between the two stars is $\Delta V = 3.10$ mag (Table 4). Bolometric corrections and the temperature calibration for the spectral type B3.5 V are taken from Flower (1977). Table 5 lists these values for S Mus B. For comparison, similar parameters are also listed for B3 V and B4 V stars. From the discussion in the preceding sec-

TABLE 5. The companion of S Mus.

Companion	$\log T_{\rm eff}$	$T_{\rm eff}$ (K)	B.C. com (mag)	V_0 com (mag)	$\Delta M_{\rm bol}$ com−Cep (mag)	$\log L_{\rm com}$ ($L_\odot$)
B3.5 V	4.251	17 800	−1.71	8.57	1.40	3.00
B3.0 V	4.273	18 700	−1.84	8.58	1.28	3.05
B4.0 V	4.229	16 900	−1.58	8.56	1.52	2.95

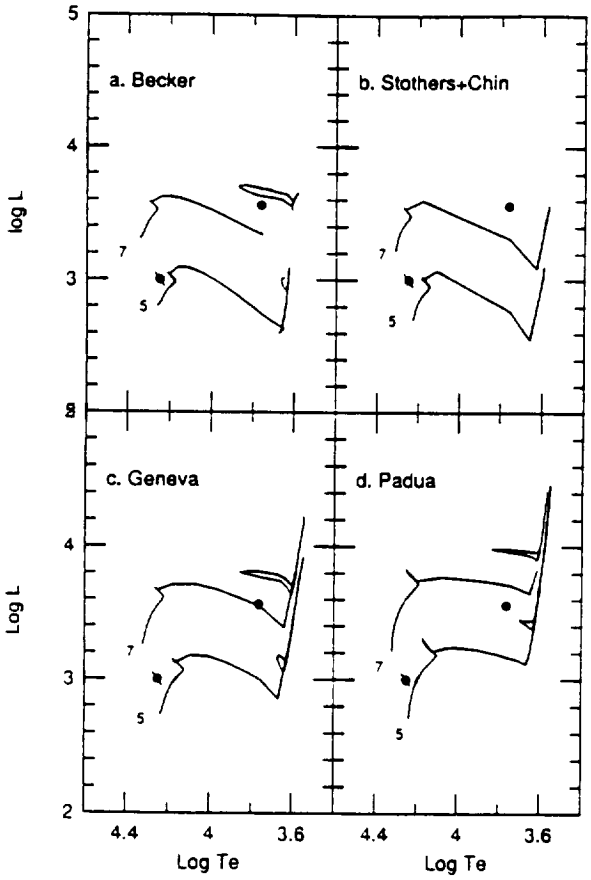

FIG. 7. S Mus A and B compared with evolutionary tracks for 5 and 7 $\mathcal{M}_\odot$ stars computed by four groups. The error bars for S Mus B indicate the locations of B3 V and B4 V stars (Table 5). Masses in $\mathcal{M}_\odot$ are indicated to the left of each track. Luminosities in all figures are in $L_\odot$. (a) Tracks from Becker. (b) Tracks from Stothers and Chin. (c) Tracks from the Geneva group. (d) Tracks from the Padua group.

tions, S Mus B lies between these two spectral types, so these values provide uncertainties for $\log T_{\rm eff}$ and $\log L$. Table 5 shows that although V_0 of the companion depends on the spectral type, the variation is insignificant.

The temperature for B3.5 V in Table 5 is in reasonable agreement with that determined directly from the *IUE* spectra (Fig. 6) as discussed above, although a precise temperature determination is not possible from this approach because of the differences between the models and observations. The temperature in Table 5 is in very good agreement with the temperature from Böhm-Vitense & Proffitt (1985) from older Kurucz models.

Using these values of luminosity and temperature, we can compare the components of the S Mus system with evolutionary tracks. Figure 7 shows this comparison for the tracks computed by several groups. While all are compositions close to $Y=0.28$ and $Z=0.02$, they differ in several ways. The tracks by Becker (1981) and those of Bertelli *et al.* (1986) use versions of Los Alamos opacities. The tracks of Stothers & Chin (1991a) and Schaller *et al.* (1992) use newer opacities, for example, those of Iglesias *et al.* (1992). (The tracks of Bertelli *et al.* will be referred to as the Padua group below; those of Schaller *et al.* will be referred to as the Geneva group.) A far more significant difference in the calculations is the treatment of the convective core boundary in main sequence stars. Becker and Stothers and Chin assume that there is no convective overshoot at this boundary; the Geneva group include a moderate amount of overshoot; the Padua group use the largest value.

The first result from Fig. 7 is that because of the relatively small luminosity difference between the two stars in the S Mus system, it cannot be assumed that S Mus B is on the zero age main sequence.

Even with the variation in codes and parameters, the location of S Mus B in all four sections of Fig. 7 corresponds to a small range in masses. For all tracks, the mass is between 5.5 and 6.0 $\mathcal{M}_\odot$. (Half a solar mass is also about the range allowed by the error bars from the possible range in spectral types.)

On the other hand, the evolutionary state of S Mus B (whether it is near the beginning or end of its main sequence lifetime) is quite different for the four sets of tracks. Those with little overshoot (Becker, Stothers and Chin) place S Mus B in the middle or toward the end of its main sequence lifetime. As the importance of overshoot increases, S Mus B is found closer to the beginning of its main sequence phase.

Within a binary system, the magnitude difference between the two components can also be compared with the mass difference implied by the tracks, and the position of the companion within the main sequence. The mass difference of approximately one solar mass implied by the Becker, and also the Stothers and Chin tracks is consistent with a companion well into its main sequence lifetime. [In the case of the Stothers and Chin tracks, this assumes that there are a number of ways of "triggering" blue loops, such as downward overshoot from the outer convective envelope, as discussed by Alongi *et al.* (1991) and Stothers & Chin (1991b). In Fig. 7(b), for instance, blue loops could be produced using reasonable parameters.] Both the Geneva tracks and the Padua tracks imply mass differences less than a solar mass, and yet the companion is only at the beginning of its main sequence phase. For the Padua tracks, the Cepheid and the companion have essentially the same mass, which is incompatible with quite different states of evolution.

This comparison between tracks with varying amounts of overshoot is also displayed in Fig. 8, using isochrones. In Fig. 8(a), The middle isochrone (age 39×10^6 yr) has the right temperature for the companion as well as the right luminosity for the Cepheid (assuming the "kink" in the giant region could be made to extend horizontally into a blue loop as discussed in the previous paragraph). In the Geneva isochrones, however, a single isochrone is a poor fit to S Mus A and B since the Cepheid is much less luminous than the isochrone with the temperature of the companion.

In summary, the mass of S Mus B is a very robust result, being 5.5 to 6.0 $\mathcal{M}_\odot$ for evolutionary tracks from a wide range of codes. On the other hand, only the tracks with minimal convective overshoot show a consistent picture between a reasonably small luminosity difference between the two stars and a main sequence star approaching the end of the main sequence band.

Since one of the main aims of investigating the temperature and mass of S Mus B is to use it to determine the mass of the Cepheid, it may seem that the use of the Cepheid

The Temperature of the Supergiant α Per [1]

Nancy Remage Evans

Department of Physics and Astronomy, York University, 4700 Keele St., North York, Ontario, M3J 1P3, Canada

Terry J. Teays [2] and Lyla L. Taylor [2]

Computer Sciences Corp., Center for Scientific Research, Science Programs, 10000 A Aerospace Rd., Lanham-Seabrook, MD, 20706

John B. Lester

Department of Astronomy, Erindale College, University of Toronto, Mississauga, Ontario, L5L 1C6, Canada

Robert B. Hindsley

Astronomy Department, US Naval Observatory, 3450 Massachusetts Ave., NW, Washington, DC, 20374

Abstract.

We compare observed fluxes from the ultraviolet (IUE) through J and K with recent Kurucz model atmospheres to determine a temperature for the F5 Ib supergiant α Per. The two most important advances in this study as compared with previous work are the use of well calibrated ultraviolet fluxes and the use of models with an appropriate microturbulence.

1. Introduction

There are many questions in astrophysics which require a temperature derived from the entire spectral energy distribution. As a first step in determining a temperature scale for Cepheids and non-variable supergiants, we have determined the temperature for the F5 Ib supergiant Alpha Per.

2. Data

Observations of α Per, as well as a number of other nonvariable supergiants, have been assembled including International Ultraviolet Explorer satellite (IUE)

---

[1] IUE Archival Research

[2] Staff Member of the International Ultraviolet Explorer Observatory

spectra and B, V, R, I, J, and K as discussed by Evans, et al. (1993). Because α Per is located in a cluster, and because its angular diameter has been measured, its log g is known observationally, as is the microturbulence in the atmosphere. We adopt a reddening E(B–V) = 0.04 mag from the stars closest to α Per in the cluster (Gray, 1991). These data are discussed in detail by Evans, et al. (1995), as is the process of determining the temperature.

3. Models

The observed energy distribution of α Per was compared with model atmospheres consistent with the observed values of gravity and microturbulence. Because supergiants have microturbulence higher than the standard value of 2 kms^{-1}, one of us (JBL) computed a series of fully line blanketed model atmospheres using the Atlas 9 code of Kurucz. For the broad-band comparisons, the model atmospheres were convolved with standard filter sensitivity functions (Evans, et al. 1995). The ultraviolet flux is sensitive to gravity and microturbulence, as well as temperature. Because we cannot resolve this degeneracy using the energy distributions, we fix log g at 1.5 and microturbulence at 4 kms^{-1} (as observed), and derive the temperature from the best fit to the energy distribution (6270 K).

4. Discussion

The rms deviation to the fit (0.065 mag) is reasonable considering that the data are assembled from many sources which are calibrated in different ways. This uncertainty corresponds to a temperature range of $\pm$ 120 K. The temperature derived from the distance to the cluster and angular diameter is within this range. Temperatures have recently been determined in several studies using the infrared flux method (Blackwell, et al. 1991, McWilliam, 1991). The differences in the temperatures between this study and the others can be attributed to the different reddenings.

Acknowledgments. Financial support was provided by a Natural Sciences and Engineering Research Council (Canada) grant to NRE and JBL and a NASA grant NAS5-31845 to TJT. Computing facilities were furnished by Dr. J. J. Caldwell at York University.

References

Blackwell, D. E., Lynas-Gray, A. E., and Petford, A. D. 1991, A&A, 245, 567

Evans, N. R., Jiang, J. H., McAlary, C. W., and Campins, H. 1993, AJ, 106, 726.

Evans, N. R., Teays, T. J., Taylor, L. L., Lester, J. B., and Hindsley, R. B. 1995 submitted to AJ

Gray, R. O. 1991, A&A, 252, 237

McWilliam, A. 1991, AJ, 101, 1065

The Temperature of the Supergiant α Per [1]

NANCY REMAGE EVANS
Department of Physics and Astronomy
York University, 4700 Keele St., North York, Ontario M3J 1P3, Canada

TERRY J. TEAYS[2] and LYLA L. TAYLOR[2]
Computer Sciences Corp.
Center for Scientific Research, Science Programs
10000 A Aerospace Rd. Lanham-Seabrook, MD 20706, USA

JOHN B. LESTER
Department of Astronomy
Erindale College, University of Toronto
Mississauga, ON, L5L 1C6, Canada

ROBERT B. HINDSLEY
Astronomy Department, US Naval Observatory
3450 Massachusetts Ave. NW, Washington, DC 20372, USA

Received:

Accepted:

Address for Correspondence:
Nancy R. Evans
Department of Physics and Astronomy
c/o CRESS
York University
4700 Keele St.
North York, Ont. M3J 1P3, Canada
email: evans@nereid.sal.ists.ca

[1] IUE Archival Research

[2] Staff Member of the International Ultraviolet Explorer Observatory

Abstract

Because the bright supergiant α Per is located in cluster, and because its angular diameter has been measured, its log g is known observationally, as is its atmospheric microturbulence. Using these observed parameters, we compare its energy distribution derived from IUE spectra and B, V, R, I, J, and K with model atmospheres convolved with instrumental sensitivity functions. The two most important advances in this study as compared with previous work are the use of well calibrated ultraviolet fluxes and the use of models with an appropriate microturbulence. Because the ultraviolet flux is sensitive to log g and microturbulence, as well as temperature, we fix log g at 1.5 and microturbulence at 4 km sec^{-1}, and derive the temperature from the best fit to the energy distribution (6270 K). Other recent temperature determinations are discussed, as are the sources of error.

1. Introduction

This paper is part of an ongoing series of investigations into the energy distributions of classical Cepheids and nonvariable supergiants. In the first paper of the series, Evans, *et al.* (1993, called Paper I below) assembled data from the ultraviolet through the near infrared, including International Ultraviolet Explorer (IUE) satellite spectra, and B, V, R, I, J, H, and K photometry. (Further discussion about the G8 Ib supergiant HR 9053 is provided by Evans *et al.* [1994]). In addition to discussing the reddening law and calibration of the photometry, Paper I also made comparisons of the energy distributions for nonvariable supergiants and pulsating Cepheids. In general the energy distribution for δ Cep is identical to that of a nonvariable supergiant with the same $(B-V)_0$. However, there are two exceptions. First, at its the hottest phases, δ Cep has too much ultraviolet flux as compared with the nonvariables. Second, at the "piston phase" of its pulsation δ Cep has too much ultraviolet flux, even in comparison with other phases.

Specifically, this approach lets us investigate how accurately the energy distribution of a supergiant (ultimately a pulsating supergiant) can be matched with a plane parallel static atmosphere model described by four parameters T_{eff}, log g, microturbulence, and an assumed solar abundance. The model atmospheres may not represent the observations perfectly, since α Per and the other supergiants we will discuss in subsequent papers are certainly extended. However, at least these stars are apparently not losing mass.

The application of the infrared flux method (IRFM) to determine Cepheid radii and temperatures (Fernley, Skillen, and Jameson, 1989) provides an example of the value of investigations of the overall energy distributions. Comparing the observed ratio of flux in the infrared region (relatively insensitive to temperature) to total

flux from observations with the same ratio from model atmospheres determines both the temperature and the angular diameter in an iterative way. Clearly, the atmospheres used must accurately represent the stars, which we will investigate in this study.

To continue this series of investigations, we will now compare the observed energy distributions with computed model atmospheres to see how well the energy distribution (which includes nearly all the energy from these stars) can be represented by static atmospheres. As the first step in this investigation, we begin with α Per, a bright, well studied supergiant. Furthermore, because it is a member of a cluster, its reddening, absolute magnitude and mass can be derived observationally. It also has angular diameter measurements. This allows us to constrain its gravity in a direct way for comparison with the results from the atmospheres.

2. Observed Parameters of α Persei

In this section, we will summarize the observed parameters of α Per.

Reddening: Alpha Per is the brightest star in the well-studied cluster of the same name. There is general agreement that there is some differential reddening in the cluster (e.g. Turner, 1976), as is indicated by the width of the main sequence (Mitchell, 1960). A recent study by Gray (1991) finds an E(B–V) = 0.04 mag from the stars closest to α Per (using E(b-y) = 0.78 E(B–V) from Fernie, 1987). A similar conclusion was reached by Crawford and Barnes (1974), even though this is smaller than the average value for the cluster. This is the same value derived by Parsons and Bell (1975) from multicolor photometry.

Distance: The true distance modulus to the cluster was determined by Crawford and Barnes to be V_0–M_V = 6.1 mag and by Turner to be 6.02 mag. In a recent

discussion of cluster isochrones, Meynet, Mermilliod, and Maeder (1993) use V_0–M_V = 6.08 mag. If we adopt the Meynet *et al.* value as being representative, the absolute magnitude of α Per becomes -4.4 mag (corrected for its individual reddening) and the distance to the cluster becomes 164 pc. An uncertainty in the distance modulus of ± 0.1 corresponds to an uncertainty in the distance of ± 8 pc

Mass: Meynet *et al.* derive an age for the α Per cluster of 52 × 10^6 years by fitting their isochrones. This isochrone provides a mass of α Per itself of 6.6 $M_\odot$. These isochrones use recent opacities and a modest amount of convective overshoot at the main sequence core boundary. To give a sense of the dependence of this mass estimate on the physical inputs, the evolutionary tracks of Becker, Iben, and Tuggle (1977) for the same abundance but no convective overshoot (and old opacities) predict a mass of 7.2 $M_\odot$.

Angular Diameter: Angular diameter measurements of α Per are benefiting from the continuous improvements in instrumentation. Currently available measurements are 3.20 ± 0.25 mas (Koechlin and Rabbia 1985) and 2.9 ± 0.4 mas (Bonneau, *et al.*, 1981). Early Mark III interferometer measurements were larger (5.0 ± 0.5 Shao *et al.* 1988), but more recent Mark III measurements are in good agreement with the smaller results (Mozurkewich, 1994). Therefore we will adopt the Koechlin and Rabbia result, which is in good agreement with the recent Mark III results.

Radius: The radius of α Per can be derived from these results in two ways. First if we assume a reasonable range of temperatures (to be confirmed by this study), we can combine the temperature with the luminosity to derive a radius. (A bolometric correction is taken from Flower, 1977). The temperatures 6400, 6300, and 6200 K correspond to radii of 52, 54, and 56 $R_\odot$ respectively. An added

uncertainty in distance modulus of $\pm$ 0.1 increases the total range of radii from 50 to 59 $R_\odot$.

Alternately, the angular diameter can be combined with the distance to provide a radius. From this approach the radius is 56 $R_\odot$, in good agreement with the one in the preceding paragraph. The ($\pm$ 1 σ) values of angular diameter and distance result in a radius range from 50 to 63 $R_\odot$.

Gravity: From the above information, log g = 1.7 $\pm$ 0.1 cm sec^{-2}, for R = 56 $R_\odot$ and a range of masses of 5 to 7 $M_\odot$. This uncertainty is doubled for the range of masses and extreme radii.

Microturbulence: The final parameter needed for comparison with model atmosphere calculations is the microturbulence. Luck and Lambert (1985) find a microturbulence of 3.0 km sec^{-1} for α Per. Spaan et al. (1987) summarize previous values and find 6.0 km sec^{-1} from visual data and 5.1 km sec^{-1} from ultraviolet data. In this study we will use 4.0 km sec^{-1} as a reasonable summary of previous data. As for other supergiants, it is larger than the standard value of 2 km sec^{-1} which is the default value in Kurucz (1991) calculations.

3. Details of the Process

Calibration: The aim of this investigation is to compare the observed fluxes as discussed in Paper I with those predicted by the recent Kurucz models. As in Paper I, the fluxes are a combination of IUE observations and calibrated ground-based broad-band fluxes. The calibrations are the ones given by Fernley, Skillen and Jameson (1989) except that the correction factor to remove the spectral type dependence of the calibration has not been included, since the comparisons are between the observed data and filter/model convolutions. In recent years, a great

deal of work has gone into standardizing infrared color systems (Bessell and Brett, 1988). In addition, there have been several discussions of the infrared calibration (Blackwell and Lynas-Gray, 1994; Cohen, et al., 1992; Alonso, et al., 1994). The calibration adopted by Fernley, Skillen, and Jameson (1989) is in good agreement with these studies and is used in this and future studies. It is also very similar to that of Campins, et al. (1985) which was used in Paper I.

Filter Functions: The fluxes from Kurucz model atmospheres were convolved with filter sensitivity functions to create colors that were then compared with the observed fluxes. The filter sensitivity functions were taken from the following sources: B and V: Buser and Kurucz (1978), I_C and R_C: Bessell (1990), and J, H, and K: Bessell and Brett (1989).

Models: For supergiants it is important to use a microturbulence higher than the standard value of 2 km sec^{-1}. One of us (JBL) computed a series of fully line-blanketed model atmospheres using the Atlas9 code. The grid includes for an appropriate range of temperature (in steps of 500 K), log g (in steps of 0.5), and microturbulence of 2, 4, and 8 km sec^{-1}. For the comparisons with the observations, fluxes from these models were linearly interpolated within this grid to smaller steps in temperature. After these calculations were completed, Kurucz distributed models and fluxes for the range of microturbulences treated here, and the fluxes agree closely with ours.

Vega and the Sun: The following check was performed to confirm that our approach works for both the standard calibrating star, Vega, and also the sun, which is similar in temperature to α Per and the other yellow supergiants we will analyze in subsequent studies. Table 1a contains the observed colors of Vega from Fernley, Lynas-Gray, et al. (1989), together with the calibrated flux ratios (with

respect to V). In addition, same flux ratios have been derived by convolving the filter functions with the Kurucz model of Vega (T_{eff} = 9400 K, log g = 3.95, log abundance with respect to solar abundance = 0.0). The final column shows the difference between the observed and computed flux ratios. This is the atmosphere used by Kurucz (1991) as the best match to the visual observations, even though he recognizes that Vega's abundance is not strictly solar.

Solar colors are difficult to determine, and have been the subject of considerable controversy. A consensus seems to be emerging that the sun lies between 16 Cyg B and 16 Cyg A in color (e.g. Garrison, 1993; Friel, et al., 1993, Neckel, 1986) In Table 1b we compare the colors of 16 Cyg A and 16 Cyg B with colors derived from other analyses of solar analogs. The B, V, R, I, colors of 16 Cyg A and 16 Cyg B are taken from Moffett and Barnes (1979). The Johnson R and I are transformed to the Cousins system using the equations provided by Fernie (1983), as was done with data in Paper I. V–J and V–K were taken from Johnson, et al. (1966). For comparison, the final column in Table 1b shows solar colors derived from the means of a number of solar analogs. J, H, and K are taken from Campins, et al. (1985). B, R, and I are taken from Bessell and Norris (1984).

Table 1b shows that indeed, the derived solar colors fall between the observed colors of 16 Cyg A and 16 Cyg B. The exception is B–V, which is slightly redder than either of the comparison stars. Because of this [and because of other recent results, including Taylor (1994)], we will adopt B–V = 0.65 mag for the sun.

The colors from the final column in Table 1b have been calibrated and compared with model results in the same way as Vega observations in Table 1a. (The solar model used for comparison had a temperature of 5770 K and log g of 4.44.)

The final column of Table 1a gives an estimate of the uncertainty which results from this approach, even for two stars where the models have been carefully matched to a wide variety of observations. This uncertainty includes errors in data measurement, filter response functions, and model calculations (including the improved opacities in the new models). For both stars, the B filter has the largest difference between the observed and computed fluxes. This region of the spectrum contains numerous and strong absorption features as well as an overall energy distribution with a large variation in flux levels from the shortest to the longest wavelength. It is not surprising that it is difficult to reproduce this broadband color. As a working model (partly because of preliminary investigations with supergiants), we will adopt a small correction to the computed log Flux(B) - log Flux (V) = 0.04 to be added to the computed flux.

Ultraviolet Fluxes: As in Paper I, the IUE spectra were binned into 100 Å bins, which can be directly compared with comparable bins from the models. Bins 100 Å wide are small enough to preserve the details of the ultraviolet continuum, but large enough to give a reliable mean flux.

Weighting Scheme: The observed and model fluxes are compared in an RMS minimization scheme in order to have an objective determination of goodness of fit. As part of the fitting, for each comparison, the mean offset between the two energy distributions was varied so that the best match (smallest rms) could be identified.

Weights were assigned to each flux band. The 100 Å ultraviolet bands were given a smaller weight (0.5) than the broad bands in the visible and near infrared (weight 1.0). Experience showed that some of the IUE bins had systematically large differences between the observations and the models. Specifically, observed flux from 2750 to 2850 Å and from 2350 to 2450 Å is larger than the computed

flux. Inspection of the spectra showed that the former is dominated by very strong absorption lines (Mg II h and k) or and the latter by a strong absorption band. Because these bins are the likely to be affected (in the sense observed) by scattered light in cool star spectra and the models cannot be expected to reproduce any chromospheric contributions (Mg II h and k), these bins were given zero weight.

A more important distinction between wavelength regions became important in the course of this project. In addition to the IUE spectra from 2000 to 3200 Å, short wavelength IUE spectra were also obtained for α Per, the other nonvariable supergiants and also for δ Cep. Fluxes for bands from 1750 to 1850 Å and 1850 to 1950 Å were determined from these. The observed fluxes for α Per and the other nonvariable supergiants were systematically larger than the computed fluxes. The explanation is contained in a recent paper by Morossi, et al. (1993). In a study of late G and K stars (primarily giants and supergiants), they found excess flux in the IUE energy distributions. For the coolest stars, the whole wavelength range shorter than 3000 Å was affected, but for $T_{eff} \geq 5000$ K, the effect was only prominent for wavelengths shorter than 2500 Å. Their interpretation was that the shortest wavelengths showed the effects of a non-radiative source of heating.

Since α Per is hotter than 6000 K, the effect should only be found at even shorter wavelengths, in particular the SWP fluxes. (This effect is much larger than the scattered light known to effect IUE spectra of late type stars.) As a precaution only fluxes at wavelengths longer than 2550 Å were used.

An interesting result of this series of studies will be to trace the occurance of this heating in supergiants as a function of temperature, and to compare its prominence in Cepheids and nonvariables.

4. Results

Because α Per is the first star we have investigated, and also because its physical parameters are better known than those for any other supergiant, we present Figures 1, 2, and 3 to illustrate the changes resulting from changes in T_{eff}, log g, and microtubulence close to the optimum values. (Much wider ranges of the parameters were explored than are presented in Figures 1 to 3.)

The patient reader can also use Figures 1 to 3 to confirm that the region most sensitive to the parameter changes is the IUE region (2500 to 3200 Å). Hence it is this region that dominates the changes in the computed fit of the energy distribution.

The physical parameters controlling the region from 2500 to 3200 Å, however, are not simple to disentangle. A comparison of 1c, 2c, and 3c, for instance, shows that this region is also sensitive to the microturbulence. On the other hand, comparison of 2a and 2c shows that a change in gravity produces a similar variation in the ultraviolet flux. In other words, there is a degeneracy between gravity and microturbulence in the energy distribution. However, as discussed in section 2 above, from other measurements, we have good determinations of these parameters. Therefore, we have proceeded as follows. We adopt log g = 1.5 and microturbulence = 4 km sec^{-1}. While these may not be exact values, we cannot refine them further from the energy distribution. Small changes to one parameter could be compensated by the other. We can then interpolate between models to find the optimum temperature. In the case of α Per, 6250 to 6300 K is the best fit (Figs. 2c and 2d).

Figure 1 can also be used to confirm:

- Extra flux is observed for wavelengths shorter than 2000 Å as compared with the model (the two shortest wavelength points).

- Without the small flux correction to B, the difference between observed and

computed would be larger: i.e. the correction is consistent with the α Per results.

• While good fits can be produced with a microturbulence of 2 km sec^{-1}, the fits with 8 km sec^{-1} are always poor.

In summary, although using a least squares criterion for the energy distribution alone would result in different parameters (for instance a smaller gravity), the combination of external constraints provides a temperature of 6250 to 6300 K for α Per. Furthermore, the energy distribution is satisfactorily fit with this temperature and log g = 1.5 and microturbulence = 4 km sec^{-1}; although this fit is not unique.

Because this is the first star we have investigated, we present Table 2 containing rms deviations to provide further insight into the fittings. The deviations are shown for a small region of temperature which contains the best fit for the adopted valued of log g = 1.5 and microturbulence = 4 km sec^{-1}. For convenience, the minimum deviation is asterisked in each column for each microturbulence (for this temperature range). It is clear that very different "best fit" temperatures are obtained (for instance log g = 1.5) for different values of the microturbulence.

5. Discussion

The standard deviation values in Table 2 can be compared with the errors estimated to be present in the data. The minimum value 0.026 log flux corresponds to 0.065 mag. This is similar in size to the errors given in Table 1a for the sun and Vega. Among errors present in the data are observational errors, errors in the calibration of the broad band fluxes and the IUE fluxes, errors in the models, and errors in the instrumental sensitivity functions. Fernley, Lynas-Gray, et al. (1989) estimate a $\pm$ 3% error in the infrared calibrations. The error in the absolute IUE fluxes is at least that large, but a systematic error in the IUE fluxes would probably

result in the selection of a different temperature rather than an increase in the s.d. Photometric errors in the absolute broad-band photometry can easily be 2%. Photometric errors in the infrared photometry are somewhat larger. The scatter in repeated IUE observations binned into 150 Å bins is comparable (Garhart, 1992). In summary, the minimum deviation in Table 2 can be accounted for by errors to be expected from photometric and calibration errors, and provides no reason to conclude that the model does not adequately represent the observations.

On the other hand, Table 2 also illustrates that the error in the fit only increases slowly away from the best fit. A quadratic fit to Table 2 results in a temperature of 6270 K for microturbulence = 4 km $\quad \sec^{-1}$ and log g = 1.5. We will assume that the error in the temperature can be estimated from the error in the mean computed from the fit (σ) of the energy distribution (Table 2) which is derived from 11 datapoints ($\sigma/\sqrt{(11)}$. Using the minimum σ in Table 2 (0.026), we then look for temperatures in Table 2 with σ = 0.026 + 0.008. In Table 2, this corresponds to a temperature range of ± 120 K.

The temperature we have found depends heavily on the reddening we adopted, E(V–B) = 0.04 mag. To investigate the sensitivity of the temperature to the reddening, we did a solution arbitrarily using a reddening of E(B–V) = 0.08 mag. The "best fit" temperature went from 6270 K to 6500 K, with an equally good fit.

We can compute a "cluster temperature" using the luminosity from the distance of α Per from the cluster and the measured angular diameter of the star. Using log $L/L_{\odot}$ = 3.62 and $R/R_{\odot}$ = 56, the temperature is 6170 K. Using ±0.1 mag as the uncertainty in the distance modulus and 0.25 mas as the uncertainty in the angular diameter leads to an error of 6% or ± 370 K in the temperature.

For comparison, other temperatures derived for α Per are collected in Table 3. Table 3a shows temperatures recently determined by the infrared flux method (IRFM) from three sources. None of these can be considered the final word since all use atmospheres that predate the most recent Kurucz atmospheres (1979 Kurucz atmospheres for McWilliam and the MARCS code [Gustafsson, et al. 1975] for both Blackwell, et al. studies.) The 1991 Blackwell, et al. study is an improved version of the earlier one primarily because of an improved treatment of H^- opacity. Taken at face value, the entries in Table 3a show that a range of temperatures is presented in recent literature. A large part of the difference, however, is due to the fact that different values of reddening were used, as listed in column 2. An estimate of the effect of the extinction can be obtained from the multiplying factors listed by Blackwell and Lynas-Gray (1994, Table 4). The decrease in the McWilliam temperature and the increase in the Blackwell group temperatures bring them into approximate agreement with the temperature in this study found using E(B–V) = 0.04 mag. In addition, Blackwell and Lynas-Gray also find that using recent Kurucz atmospheres instead of MARCS atmospheres also results in a temperature increase (of order of 50 K).

In Table 3b, temperatures computed from several recent or widely used color temperature calibrations are listed. All have been computed using E(B–V) = 0.04 mag.

6. Summary

In summary, the static plane parallel, line blanketed model atmospheres adequately represent the observations from 2600 Å through 2.2 μm for the supergiant α Per when we use observationally derived values of gravity, and microturbulence. For the adopted reddening, the temperature is in agreement with other recent de-

terminations, although they all depend on the reddening. Furthermore the quality of the fit only changes relatively slowly for changes in temperature, i.e., the temperature is not tightly constrained. The temperature found for α Per in this study is 6270 ± 120 K

It may appear that this exploration of energy distributions has been done in tedious detail. However, this is the yellow supergiant for which the mass, radius, gravity, and microturbulence can be determined observationally. Consequently the energy distribution can be compared the most thoroughly with the the model atmospheres. This is the first step in using the new models to explore the energy distributions of cooler supergiants. We will subsequently investigate how well the atmospheres represent the Cepheid δ Cep throughout its pulsation cycle and finally whether the gravity effects seen in δ Cep can also be reproduced by the static atmospheres.

Acknowledgements: This work was begun while NRE was at the Institute for Space and Terrestrial Science. It is a pleasure to thank Dr. J. Bonnell for assistance with original Kurucz models used in the analysis. Computing facilities for NRE were furnished by Dr. J. J. Caldwell at York University. Financial support was provided by a Natural Sciences and Engineering Research Council (Canada) grants to NRE and JBL and a NASA grant NAS5-31845 to TJT.

References

Alonso, A., Arribas, S., and Martinez-Roger, C. 1994, A&A, 282, 684

Becker, S. A., Iben, I., and Tuggle, R. S. 1977, ApJ, 218, 633

Bessell, M. S. 1990, PASP, 102, 1181

Bessell, M. S. and Brett, J. M. 1988, PASP, 100, 1134

Bessell, M. S. and Norris, J. 1984, ApJ, 285, 622

Blackwell, D. E., Petford, A. D., Arribas, S., Haddock, D. J., and Selby, M. J. 1990, A&A, 232, 396

Blackwell, D. E., Lynas-Gray, A. E., and Petford, A. D. 1991, A&A, 245, 567

Blackwell, D. E. and Lynas-Gray, A. E. 1994, A&A, 282, 899

Bonneau, D., Koechlin, L., Oneto, J. L., and Vakili, F. 1981, A&A, 103, 28

Buser, R. and Kurucz, R. L. 1978, A&A, 70, 555

Campins, H., Rieke, G. H., and Lebofsky, M. J. 1985, AJ, 90, 896

Cohen, M., Walker, R. G., Barlow, M. J., and Deacon, J. R. 1992, AJ, 104, 1650

Cox, A. N. 1979, ApJ, 229, 212

Crawford, D. L. and Barnes, J. V. 1974, AJ, 79, 687

Evans, N. R., Jiang, J. H., McAlary, C. W., and Campins, H. 1993, AJ, 106, 726 (Paper I)

Evans, N. R., Jiang, J. H., Garrison, R. F., Gray, R. O., Barnes, T. G., and Frueh, M. 1994, JRASC, 88, 155

Fernley, J. A. 1989, MNRAS, 239, 905

Fernley, J. A., Skillen, I., and Jameson, R. F. 1989, MNRAS, 237, 947

Fernley, J. A., Lynas-Gray, A. E., Skillen, I., Jameson, R. F., Marang, F., Kilkenny, D., and Longmore, A. J. 1989, MNRAS, 236, 447

Fernie, J. D. 1983, PASP, 95, 782

—. 1987, AJ, 94, 1003

Flower, P. J. 1977, A&A, 54, 31

Friel, E., Cayrel de Strobel, G., Chmielewski, Y., Spite, M., Lebre, A., and Bentolila, C. 1993, A&A, 274, 825

Garhart, M. P. 1992, IUE NASA Newsletter, 48, 80

Garrison, R. F. 1993, private communication

Gray, R. O. 1991, A&A, 252, 237

Gustafsson, B. Bell, R. A., Eriksson, K. E., and Nordlund, A. 1975, A&A, 42, 407

Johnson, H. L., Mitchell, R. I., Iriarte, B., and Wisniewski, W. Z. 1966, Comm. Lun. and Planetary Lab., 4, 99

Koechlin, L. and Rabbia, Y. 1985, A&A, 153, 91

Kurucz, R. L. 1979, ApJS, 40, 1

—. 1991. in Precision Photometry: Astrophysics of the Galaxy, A. G. Davis Philip, A. R. Upgren, K. A. Janes, eds. (Schenectady: L. Davis Press). p. 27

Luck, R. E. and Lambert, D. L. 1985, ApJ, 298, 782

McWilliam, A. 1991, AJ, 101, 1065

Meynet, G., Mermilliod, J. C., and Maeder, A. 1993, A&AS, 98, 477

Mitchell, R. I. 1960, ApJ, 132, 68

Moffett, T. J. and Barnes, T. G. 1979, PASP, 91, 180

Morossi, C., Francini, M., Malagnini, M. L., Kurucz, R. L., and Buser, R. 1993, A&A, 277, 173

Mozurkewich, D. 1994, private communication

Neckel, H. 1986, A&A, 159, 175

Parsons, S. B. and Bell, R. A. 1975 in *Multicolor Photometry and the Theoretical HR Diagram*, eds. A. G. D. Philip and D. S. Hayes, Dudley Obs. Rep., 9, 73

Shao, M., Colavita, M. M., Hines, B. E., Staelin, D. H., Hutter, D. J., Johnston, K. J., Mozurkewich, D., Simon, R. S., Hershey, J. L., Hughes, J. A., and Kaplan, G. H. 1988, ApJ, 327, 905

Spaan, F. H. P., de Jager, C., Nieuwenhuijzen, H., and Kondo, Y. 1987, A&A, 185, 229

Taylor, B. J. 1994, PASP, 106, 444

Teays, T. J., 1986, PhD Thesis, Univ. of Nebraska

Turner. D. G. 1976. AJ. 81. 1125

TABLE 1a

Vega and the Sun: Observed and Computed Fluxes

Star	Filter	Obs (mag)	Obs log (F/F_V)	Comp log (F/F_V)	O–C log (F/F_V)
Vega					
	B	0.03	0.281	0.241	0.040
	V	0.03	—	—	—
	R_c	0.04	-0.205	-0.226	0.021
	I_c	0.03_5	-0.479	-0.510	0.031
	J	0.02	-1.056	-1.064	0.008
	H	0.02	-1.477	-1.484	0.007
	K	0.02	-1.927	-1.964	0.037
Sun					
	B	0.65	0.022	-0.032	0.054
	V	0.00	—	—	—
	R_c	-0.37	-0.053	-0.072	0.019
	I_c	-0.70	-0.197	-0.216	0.019
	J	-1.12	-0.612	-0.602	-0.010
	H	-1.43	-0.909	-0.891	-0.018
	K	-1.49	-1.335	-1.351	0.016

TABLE 1b

Solar Colors

Color	16 Cyg B	16 Cyg A	Solar*
B-V	0.66	0.64	0.67
V-R_c	0.38	0.37	0.37
V-I_c	0.71	0.69	0.70
V-J	1.16	1.04	1.12
V-H			1.43
V-K	1.55	1.43	1.49

* See text for discussion

TABLE 2

Standard Deviations

log g Temperature	1.0	1.5	2.0
mt[1] = 2			
6400	0.039	0.063	0.091
6350	0.033	0.058	0.086
6300	0.028	0.053	0.081
6250	0.024*	0.048	0.076
6200	0.024*	0.044	0.071
6150	0.029	0.041	0.066
6100	0.037	0.040*	0.062*
mt[1] = 4			
6400	0.030*	0.035	0.059
6350	0.030*	0.031	0.054
6300	0.033	0.027	0.049
6250	0.039	0.026*	0.044
6200	0.047	0.028	0.041
6150	0.057	0.033	0.040*
6100	0.069	0.041	0.041
mt[1] = 8			
6400	0.064*	0.042*	0.029*
6350	0.070	0.048	0.030
6300	0.078	0.055	0.033
6250	0.088	0.064	0.039
6200	0.099	0.075	0.047
6150	0.111	0.087	0.057
6100	0.126	0.101	0.068

[1]mt = microturbulence

TABLE 3a

Temperatures of α Per

T_e K	E(B-V) (mag)	Method	Source
6516	0.10	IRFM	McWilliam 1991
6138	0.01_3	IRFM	Blackwell, et al., 1990
6154	0.01_3	IRFM	Blackwell, et al., 1991
6170	0.04	"cluster"	this paper
6270	0.04	Table 2	this paper

TABLE 3b

Color Temperatures of α Per

T_e K	Color	Source
6442	B-V	Kraft as discussed by Cox, 1979
6306	B-V	Teays, 1986
6430	V-K	Blackwell and Lynas-Gray, 1994
6300	V-K	Fernley, 1989, log g = 1.5

Figure Captions

Fig. 1 The energy distribution for microturbulence = 2 km sec^{-1}. The asterisks (stars) are the observed fluxes, scaled to V. The boxes are the fluxes from the model atmospheres. In all figures, wavelengths are in Å; fluxes are in ergs cm^{-2} sec^{-1} $Å^{-1}$. Temperature, log gravity, and microturbulence are indicated in the lower right in each graph.

Fig. 2. The energy distribtion for microturbulence = 4 km sec^{-1}. Symbols are the same as in Fig. 1.

Fig. 3. The energy distribtion for microturbulence = 8 km sec^{-1}Symbols are the same as in Fig. 1.

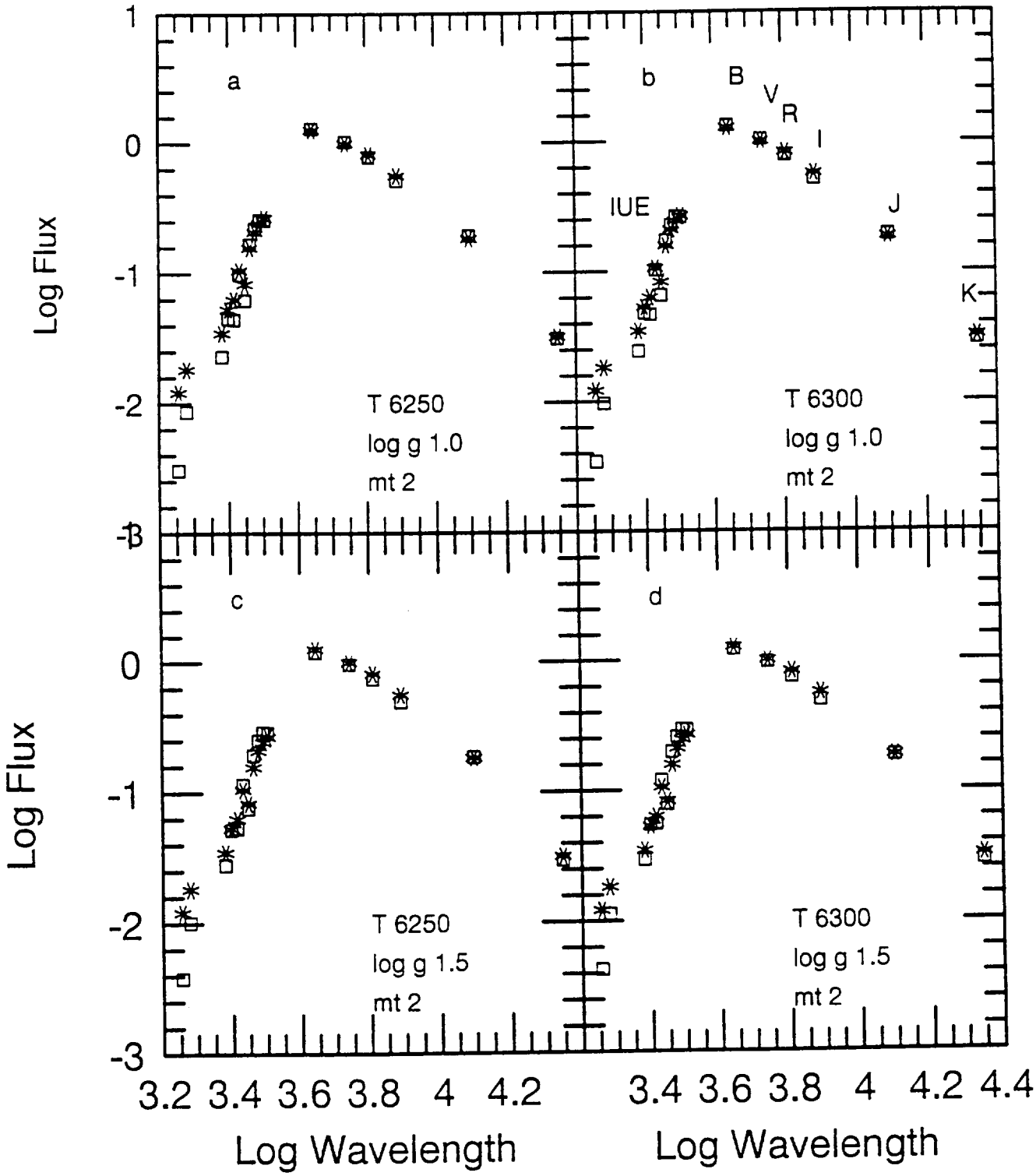
a
b
c
d
IUE
B
V
R
I
J
K
T 6250
log g 1.0
mt 2
T 6300
log g 1.0
mt 2
T 6250
log g 1.5
mt 2
T 6300
log g 1.5
mt 2
Log Flux
Log Flux
Log Wavelength
Log Wavelength
1
0
-1
-2
-3
3.2 3.4 3.6 3.8 4 4.2
3.4 3.6 3.8 4 4.2 4.4

Fig 1

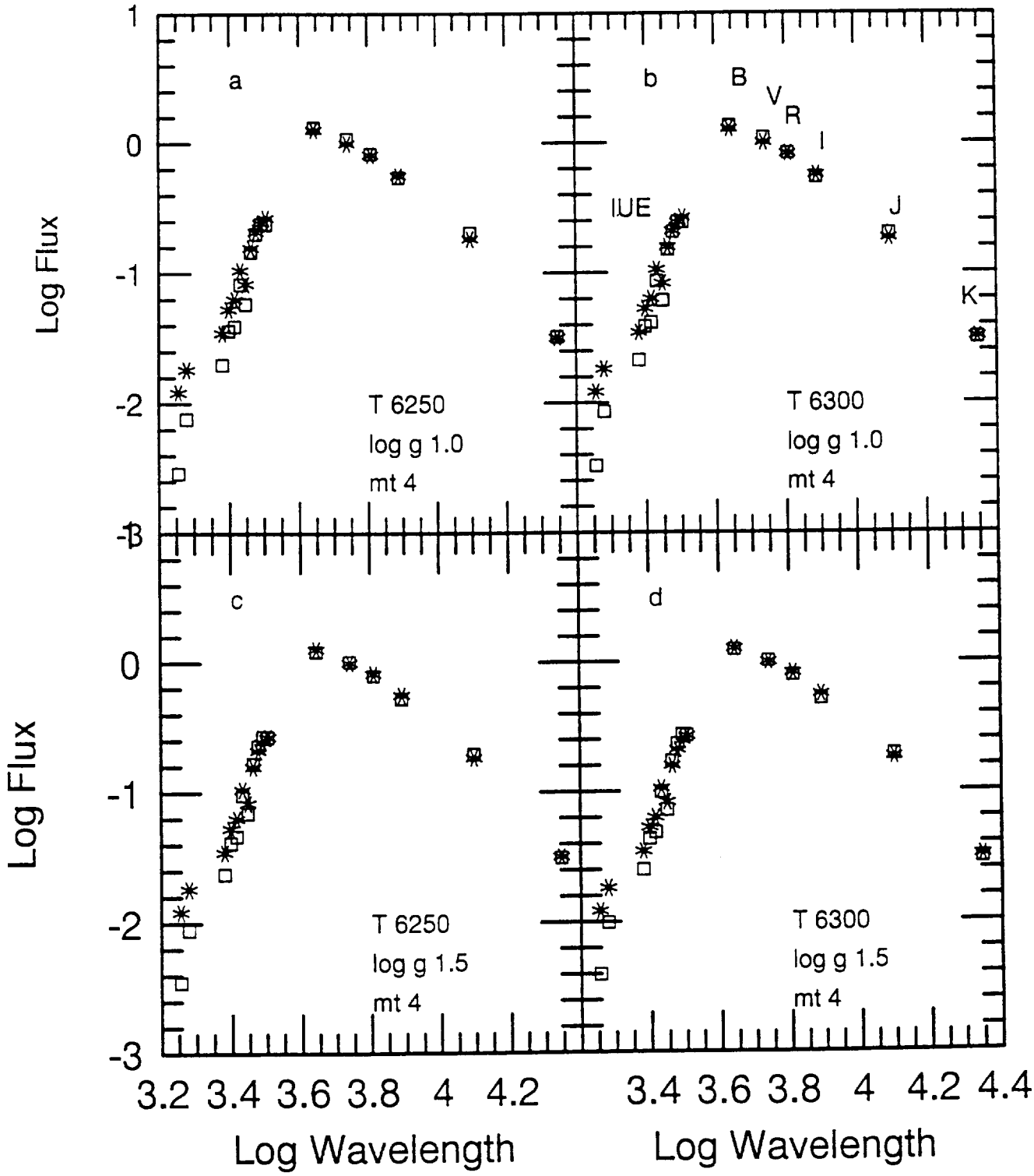
a
b
c
d
B
V
R
I
J
K
IUE
T 6250
log g 1.0
mt 4
T 6300
log g 1.0
mt 4
T 6250
log g 1.5
mt 4
T 6300
log g 1.5
mt 4
Log Flux
Log Flux
Log Wavelength
Log Wavelength
1
0
-1
-2
-3
3.2 3.4 3.6 3.8 4 4.2
3.4 3.6 3.8 4 4.2 4.4

Fig 2

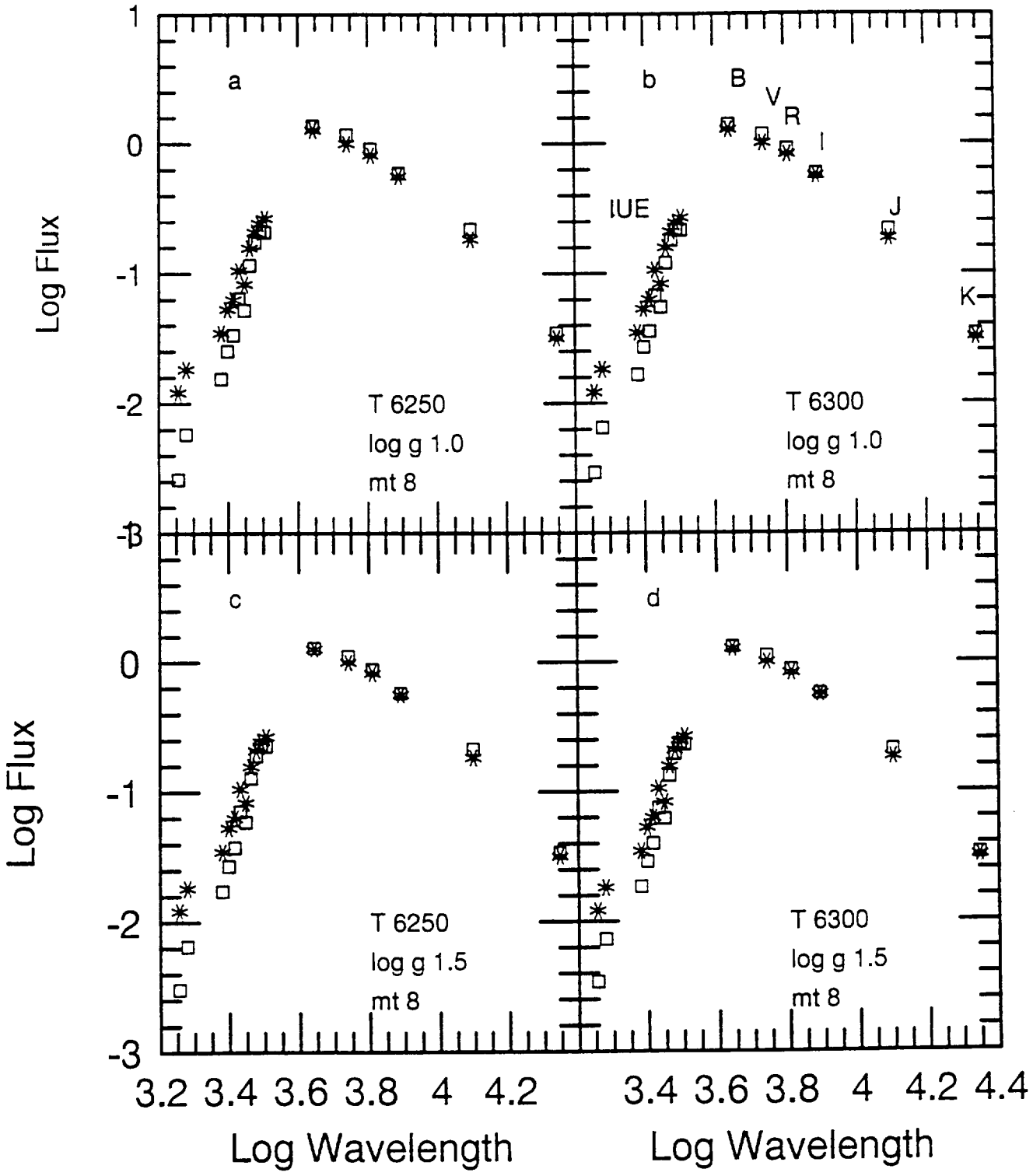
a
b
c
d
B
V
R
I
J
K
IUE
T 6250
log g 1.0
mt 8
T 6300
log g 1.0
mt 8
T 6250
log g 1.5
mt 8
T 6300
log g 1.5
mt 8
Log Flux
Log Flux
Log Wavelength
Log Wavelength
1
0
-1
-2
-3
3.2 3.4 3.6 3.8 4 4.2
3.4 3.6 3.8 4 4.2 4.4

Fig 3

125.02

First Scientific Results with the 1-m MTT Low Cost Spectroscopic Facility: Line Profile Variability in Lambda Eridanus

D.J.Barry, W.G.Bagnuolo, D.R.Gies (Georgia State University)

The Be star Lambda Eridanus was observed with the GSU 1-m Multi-Telescope-Telescope (MTT) as part of an international campaign (coordinated by R. Hirata) on four evenings (13 Nov—16 Nov UT). A full analysis of combined data from the collected observations will be presented by the team at a future date; here we derive instrumental parameters and performance for our spectroscopic facility from this first fully-operational observing run, and discuss the characteristics of profile variability derived from the observations.

125.03

New Measurements of Rotational and Turbulent Velocities for Southern Dwarfs

R.A.Osten, S.H.Saar (SAO)

We analyze high resolution ($\lambda/\Delta\lambda = 10^5$), high S/N spectra from the ESO Coudé Auxillary Telescope to derive new measurements of $v\sin i$ and macroturbulent (v_{mac}) velocities for over 50 southern dwarf stars. Five to six relatively unblended lines in each spectrum are fit with simple radiative transfer models and the results averaged to generate the final $v\sin i$ and v_{mac} values. We confirm previous results showing v_{mac} decreasing with T_{eff} for $T_{eff} \geq 5000$ K. There is some evidence that v_{mac} is enhanced in active stars, though this may be partly due to differences in atmospheric structure between these objects and inactive stars. About twenty of the stars show trends between total line velocity broadening with Landé g_{eff} implying the presence of significant magnetic flux.

125.04

A Different Emission Measure Analysis of AU Mic Flares

G. Del Zanna, B.C. Monsignori Fossi (Osservatorio Astrofisico di Arcetri), M. Landini (Dept. di Astron. dello Spazio)

On July 15, 1992, the Extreme Ultraviolet Explorer (EUVE) observed a large AU Mic flare, followed by an active phase and a second smaller flare. An analysis of the time evolution of emmission lines detected by the Short, Medium and Long Wavelength (SW, MW, LW) channels of the EUVE spectrometers has been performed. The main coronal plasma parameters as temperature, density, and differential emmission measure (DEM), during the quiet and active phases, have been deduced.

The time evolution of the differential emmission measure is provided. A high temperature component is always present in the plasma, and the DEM increases during the flares. The total emmission measures and the luminosities during the different phases are also estimated. The derived emmission measure and luminosity values are higher than the typical values for dMe flares, but similar to the large Algol flare (White *et al.*, 1986). The synthetic spectra, based on the deduced DEM distributions, and the line identifications are presented.

The physical characteristics of the events are compared with other stellar and solar data.

125.05

44i Boo (HD 133640, V=4.76) is the closest W Ma type binary star to Earth. The W Ma system (G2 V+G) is itself a member of the visual binary ADS 9494 which has a period of about 225 years (Hill *et al.* 1989, A&A, 211, 81). The visual components of ADS 9494 are currently separated by less than 3 arcseconds making it difficult to resolve from the Stephen F. Austin State University Observatory. These are compared to the extensive existing list of times of minima. Multichannel high speed photometry is used to determine times of minima in the W Ma star. Also presented are apparent rapid variations that occur out-of-eclipse. The rapid variations are analyzed with traditional period searching techniques.

125.06

CK Bootis - Starspot History as a W-type Contact Binary

N.L.Markworth (S F Austin St U)

The contact binary system CK Boo shows eclipses of almost equal depth that can change roles (primary for secondary eclipse) from one observing season to the next. Solution attempts indicate a low inclination orbit (about 60 degrees) which complicates the analysis. Markworth (1994) has presented a chronology of spotting activity on this binary which can be used to explain the changing eclipse depths. In that work the system was treated as an A-type contact system. This paper shows that a W-type solution also exists. The spotting activity needed to follow the progression of the light curve changes from year to year is once again analyzed. Although the W-type solution makes more sense in light of current thinking on contact systems and permits geometrical and astrophysical parameters that make CK Boo a much less remarkable system, the formal errors of the two solutions make them virtually indistinguishable. A modest amount of spectroscopy should be able to resolve the issue.

125.07

Photometry of the Eclipsing Binary Star MN Cassiopeiae

A.K.Sherwin, V.M.Yeager, R.J.Boyle (Dickinson College), E.B.Zamkoff (Franklin and Marshall and Dickinson Colleges)

We have observed the eclipsing binary star MN Cassiopeiae with a small format CCD and a 14 inch Schmidt-Cassegrain telescope. Our observations are in good agreement with the observations of Grauer, et. al. (1976, AJ, 8, 665). The star appears to be a β Lyrae variable composed of two very similar components with a period of 1.92 days.

125.08

A Statistical Summary for the Namelist Variables

G.G.Spear,M.Davis (SSU)

We have created machine readable versions of the namelists of variable stars as published in the Information Bulletin of Variable Stars. These lists represent stars officially designated as variables since the publication of the most recent edition of the General Catalog of Variable Stars (GCVS) as well as improved data for previously known variables. We will present a statistical summary of the namelist variables in terms of variable star types and location in the galaxy. These results will be compared with similar results for the fourth edition of the General Catalog of Variable Stars. This combined sample of GCVS plus namelist objects will be compared with those IRAS sources which were independently determined to be variable on the basis of observations by the IRAS satellite.

This research was supported by NASA grant NAG 5-1621.

125.09

Temperature Calibration of Classical Cepheids

N. R. Evans (York Univ.), T. J. Teays (Comp. Sci. Corp.)

A new temperature calibration of classical Cepheids and nonvariable supergiants has been created, based on multifrequency observations and new Kurucz model atmospheres. The data include IUE spectra from 1700 to 3200 Å and broad band B, V, R_c, I_c, J, H, and K. Variations in log g and microturbulence as well as temperature are included in the analysis. It is found that reasonable values of these three parameters represent the observed energy distributions, including the excess ultraviolet flux in δ Cep at the hottest phases. The results of this study for both nonvariable supergiants and also δ Cep are in agreement with the Kraft temperature color relation, and subsequent similar relations. The difference in non-radiative flux between Cepheids and nonvariables will be discussed. This work was supported by a Natural Sciences and Engineering Council (Canada) grant to NRE and a NASA grant NAS5-31845 to TJT.

Union are published

85

. K. Bag and

ow.

ited by R. S. Roger

off and John R. Percy.

is Johnson and Ben

of Astronomy. Edited

Developments. Edited by

by J. Nemec and

New Perspectives on Stellar Pulsation and Pulsating Variable Stars

Proceedings of IAU Colloquium No. 139
Victoria, British Columbia
15–18 July 1992

Edited by

James M. Nemec
University of Washington

and

Jaymie M. Matthews
University of British Columbia

CAMBRIDGE
UNIVERSITY PRESS

The Blazhko Effect in RR Lyrae

Terry J. Teays

Computer Sciences Corporation/IUE Observatory

Abstract

The cause of the Blazhko effect, the long-term modulation of the light and radial velocity curves of some RR Lyr stars, is still not understood. The observational characteristics of the Blazhko effect are discussed in §1. Some preliminary results are presented from aomw recent of campaigns to observe RR Lyr, using the *International Ultraviolet Explorer* along with ground-based spectroscopy and photometry, throughout a pulsation cycle, at a variety of Blazhko phases. A set of ultraviolet light curves have been generated from low dispersion IUE spectra. In addition, the (visual) light curves from IUE's Fine Error Sensor are analyzed using the Fourier decomposition technique. The values of the parameters ϕ_{21} and R_{21} at different Blazhko phases of RR Lyr span the range of values found for non-Blazhko variables of similar period.

1. Characteristics of the Blazhko Effect

The first allusion to the Blazhko effect was in a paper which included some observations of RW Draconis (Blazhko 1907) published 85 years ago, so the phenomenon has been around for a long time, and yet we still do not have an adequate understanding of it. In brief, the effect is a long term modulation of the amplitude of the light and velocity curves of an RR Lyr star. Some additional details are given below, with special focus on the properties of RR Lyr itself (the brightest RR Lyr star to show the Blazhko effect). The amplitude variation in visual light is typically quite noticeable, for example, in RR Lyr there may be a difference as large as 0.3 magnitude (out of approximately one magnitude pulsational variation), between the extremes of the Blazhko cycle. In addition the shape of the light curve varies as a function of the Blazhko cycle. [A complete set of light curves can be seen in Walraven (1949).] In RR Lyr a "shoulder" appears during rising light, just prior to maximum, in the smaller amplitude Blazhko phases, but which is not present in the larger amplitude phases. Except for this particular feature, the radial velocity curve exhibits changes which are mirror images of those seen in the light curve. In addition, emission is seen in the hydrogen lines during some Blazhko phases, but not others.

Blazhko periods (P_B) generally run from about $20 - 100^d$, i.e. $\approx$100 times the fundamental pulsation period (Π). There does not appear to be any correlation between Π and P_B (Szeidl 1988). If one compares the amplitude of pulsation for a star showing Blazhko effect to ones with a similar period that does not show it, the

Blazhko variable's amplitude at maximum most closely resembles the non-Blazhko stars (Szeidl 1988).

The amplitude of the Blazhko effect itself is also modulated on an even longer time scale in a number of RR Lyr stars. RR Lyr itself shows a tertiary period of about 3.8-4.8 years. The Blazhko effect was especially weak during 1963, 1967, 1971, and 1975. For instance, the extensive photometric and spectroscopic study of rising light performed by Preston, Smak, and Paczyński (1965) showed that the Blazhko effect was virtually non-existent in RR Lyr in 1963. Spectroscopically, the variation in the hydrogen emission strength, however, was still observable during this time.

Estimates of the percentage of RR Lyr stars which show the Blazhko effect varies in the range of 15-35%. Given that the effect can all but disappear in RR Lyr at times, as discussed above, one must view these estimates with some caution. Several Bailey Type c variables (overtone pulsators) have been proposed as stars showing Blazhko effect, but it is much harder to study in these lower amplitude pulsators with sinusoidal light curves. In general the Blazhko effect is confined to the RR Lyr stars with shorter period; it is not seen in stars with periods longer than about $0.^d6$.

2. Proposed Explanations of the Blazhko Effect

It is the characteristics that I have listed in §1 that must be explained by any theory of the cause of the Blazhko phenomenon. There is space here to only summarize the two broad categories of working hypotheses, viz., the magnetic pulsator and various resonance interactions. The former is similar to the oblique magnetic pulsator models which have been used to explain rapidly oscillating Ap stars. In theses theories P_B is just the rotation period of the star. Support for a magnetic field modulated by the pulsation and Blazhko periods has been found in the polarization measurements of Romanov, Udovichenko, and Frolov (1987). Unfortunately, the original data were not published, and these results are in need of confirmation. I would strongly urge that observers attempt magnetic field measurements of RR Lyr at a variety of pulsation and Blazhko phases. The second general class of theories proposed are those which invoke resonance interactions with other modes. Examples of these scenarios can be found in Borkowski (1980), Moskalik (1986), and Cox (this conference). None of the proposed explanations mentioned above have met with universal acceptance, due largely to their failure to account for all of the observed phenomenon.

3. The Multi-wavelength Observing Campaigns

In order to provide a fairly extensive collection of observations of the Blazhko effect I organized two multi-site, multi-wavelength campaigns during the summers of 1990 and 1991. These campaigns included ground-based photometry and spectroscopy, which was obtained to coincide with observations conducted with the *International Ultraviolet Explorer* (IUE). The IUE observations covered a complete pulsation cycle, and were repeated at a variety of Blazhko phases. The participants in this project

are:

T. J. Teays	(CSC-IUE)	J. T. Bonnell	(CSC-IUE)
T. G. Barnes III	(Texas)	J. M. Nemec	(WSU)
E. F. Milone	(Calgary)	E. F. Guinan	(Villanova)
E. G. Schmidt	(Nebraska/NSF)	J. Heath	(Texas/CalTech)
E. Poreti	(Milano-Merate Observatory)	D. G. Schleicher	(Lowell)
E. Dutchover	(Texas)	M. Frueh	(Texas)
D. Greenlaw	(Texas)	K. Venn	(Texas)

We are presently analyzing the large amount of data that were obtained during these two summers, but some preliminary results will be presented below.

a. Photometry

Ground-based photometry was obtained on a number of nights, and included (at different sites) UBVRHJK bandpasses. This photometry is being used to supplement the photometry provided by IUE's Fine Error Sensor (FES). The FES is an image dissector with an S-20 photocathode (effective wavlength = 5200 Å) which is used for target identification and tracking. It can serve as a good photometer under controlled conditions, except for the shortcoming that it provides no color information. We have used the FES to collect data during the times between taking spectra, when the spectral camera was being prepared for the next image. From these data we have constructed extensive light curves, which span a complete pulsation cycle (13.6 hours). The FES measurements have been converted into V magnitudes using the standard IUE calibration (Pérez et al. 1991). The one difficulty was in applying the correction for the (changing) color of the star. For the purposes of this paper we have made use of mean colors, calculated as a function of pulsation phase, from a model of RR Lyr by Bonnell. Figure 1 shows the FES light curves for RR Lyr at two different Blazhko phases, representing the extremes of amplitude that were observed. The Blazhko effect was clearly quite strong during the 1990 campaign!

b. IUE Observations

The 1990 campaign made use of IUE's long wavelength prime (LWP) camera in its low resolution mode, which has a wavlength range of $\approx$ 1910-3300Å. A contiguous pair of IUE shifts was used (i.e. 16 hours) in order to completely cover one pulsation cycle. Five such runs were conducted, in order to sample the Blazhko cycle in detail. The time required to read down an image on the LWP camera, and prepare the camera for the next exposure is 28 minutes. In order to increase the time resolution between subsequent spectra, we placed two spectra on the same IUE image, by offsetting them in the aperture. This technique requires additional effort beyond the usual procedures to extract the fluxes properly, but is necessary, to delineate the shape of

Figure 1. V l
IUE's FES. Thes
during the 1990 s

onnell	(CSC-IUE)
Nemec	(WSU)
Guinan	(Villanova)
h	(Texas/CalTech)
Schleicher	(Lowell)
eh	(Texas)
n	(Texas)

were obtained during
nted below.

ghts, and included (at
ng used to supplement
The FES is an image
)0 Å) which is used for
meter under controlled
olor information. We
taking spectra, when
From these data we
e pulsation cycle (13.6
magnitudes using the
y was in applying the
oses of this paper we
lsation phase, from a
ves for RR Lyr at two
le that were observed.
mpaign!

ime (LWP) camera in
-3300Å. A contiguous
ly cover one pulsation
lazhko cycle in detail.
id prepare the camera
ne resolution between
image, by offsetting
rt beyond the usual
lelineate the shape of

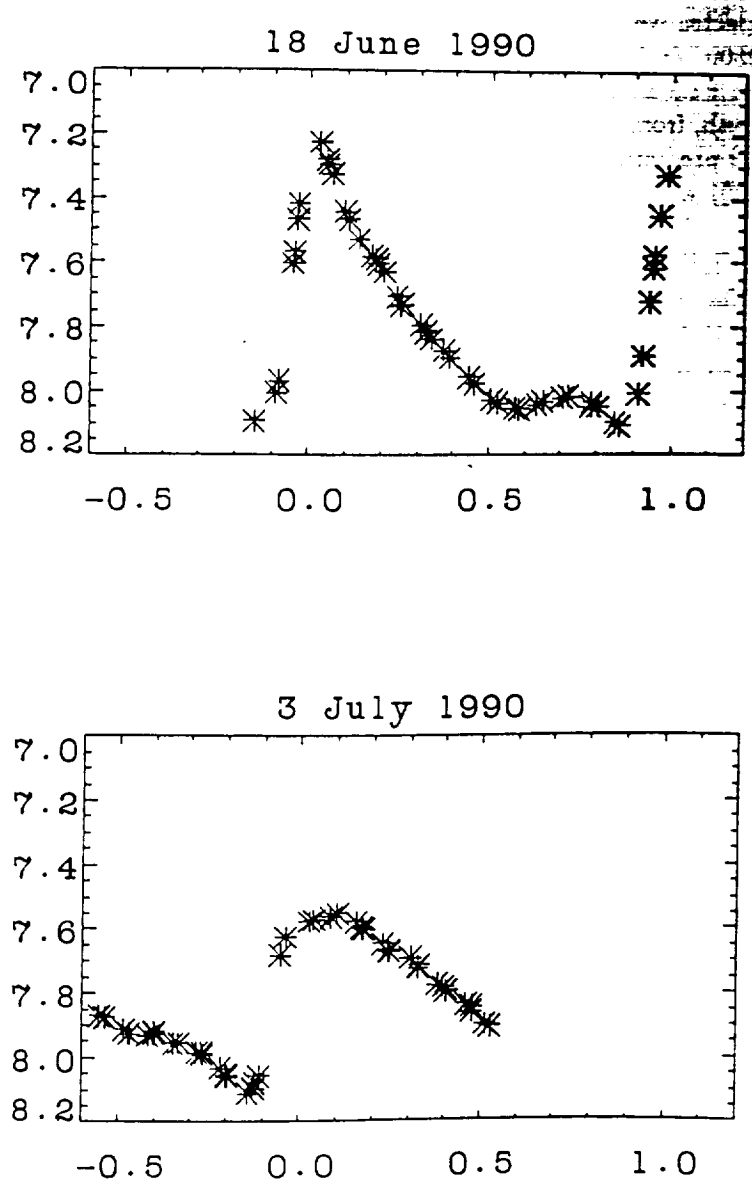

Figure 1. V light curves of RR Lyr at two different Blazhko phases, as measured by IUE's FES. These were selected to show the extremes of the variation in the light curve during the 1990 season.

the ultraviolet light curve, especially in the rapidly varying, rising light phases. From these spectra we have generated ultraviolet light curves at four wavelengths (2450, 2600, 2800, & 3000 Å) by simply binning the data. These data, when combined with the FES measurements, give the amplitude of the pulsation as a function of wavelength, from the visual through the ultraviolet, which can be directly compared to model predictions.

In 1991 we concentrated on using IUE's short wavelength prime (SWP) camera to obtain low dispersion spectra in the 1150-1975 Å range. The longer exposure times required in the SWP camera precluded us from obtaining the detailed ultraviolet light curves that we could get with the LWP camera, as well as from getting FES light curves with the necessary time resolution. Rather we concentrated on always getting a spectrum at both minimum and maximum light, so that the ultraviolet amplitude was well determined. We used four IUE shifts of eight hours duration to obtain these spectra, one of which was only two days later than a final pair of shifts that were used for obtaining detailed LWP and FES light curves, as in the 1990 campaign. This allowed us to have one time when we had complete waveleng coverage.

c. Ground-based Spectroscopy

During these campaigns spectrsocopy was obtained at McDonald, Dominion Astrophysical, and Palomar Observatories. These efforts, though hampered by the usual weather, instrument, and scheduling difficulties were successful on a number of nights. Reduction of these data is not complete, and we still have a great deal of work ahead of us to analyze the results, so in this review I will only mention the nature of the spectra taken ($\sim$ 100). Observations were concentrated on the region of the Hγ line or on the Ca II H and K lines. The former also include some metallic lines, which we can yield some radial velocity information. During the course of the pulsation cycle, one can see variable emission in the line core of Hγ.

4. Preliminary Results

The ultraviolet light curves obtained from the LWP camera have sufficient quality and phase coverage that we have been able to apply the standard Fourier decomposition techniques first introduced in Simon & Lee (1981). In addition, we have Fourier decomposed the V light curves obtained from the FES. In Figure 2 we plot the Fourier parameter ϕ_{21} vs. Π for RR Lyr at the different Blahzko phases which we sampled, and compare it to the sample of field RR Lyr stars used by Simon and Teays (1982). Similarly, Figure 3 shows the Simon & Lee parameter R_{21} plotted against period. What is seen in both cases is that the values for RR Lyr fall closely within the range of values for the non-Blazhko stars with similar pulsation period. In fact, **as RR Lyr goes through its Blazhko cycle its light curve recapitulates the appearance of all field RR Lyr stars of similar period.** We have also examined a period vs. amplitude diagram using the FES data, and confirm the results mentioned in Szeidl (1988), namely, that the closest match between Blazhko and non-Blazhko stars occurs

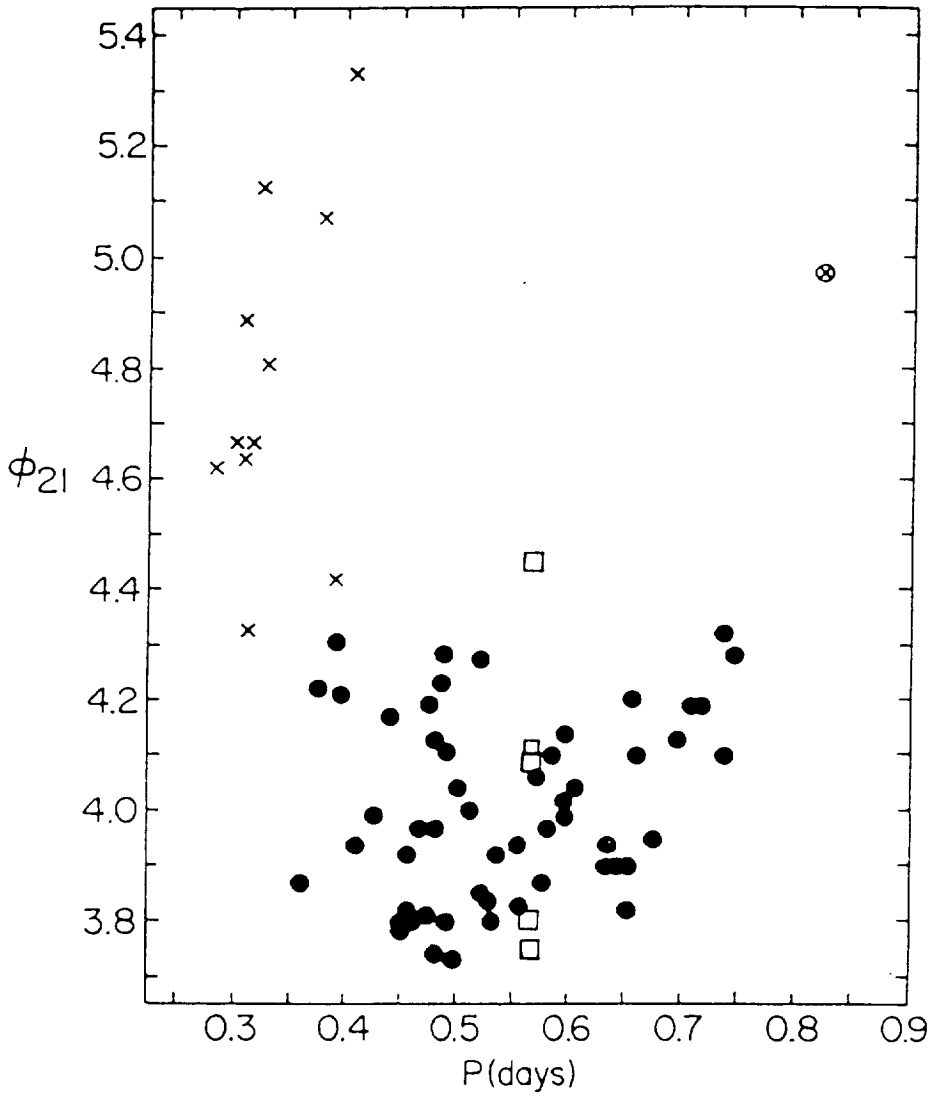

Figure 2. The Fourier decomposition parameter ϕ_{21} vs. period for non-Blazhko field RR Lyr stars (filled circles) and RR Lyr (open squares) at various Blazhko phases. The Fourier parameters are those defined by Simon & Teays (1982). (Crosses represent overtone pulsators)

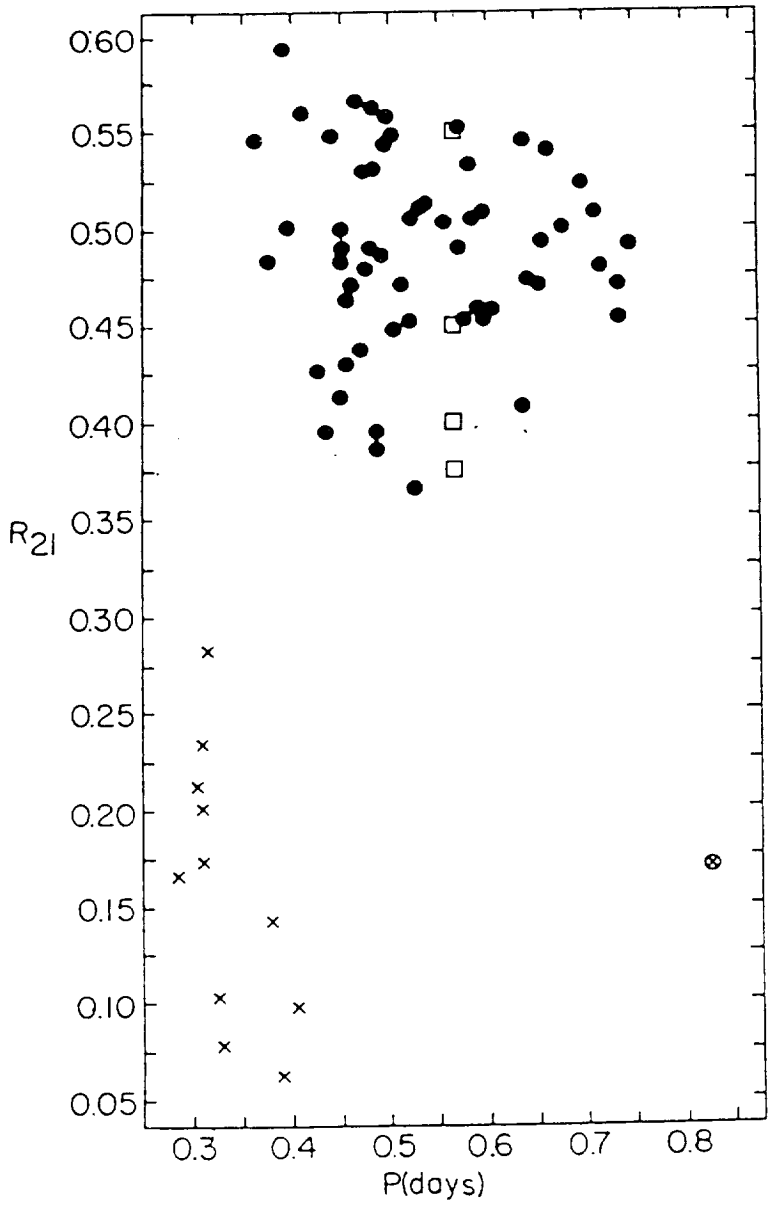

Figure 3. The Fourier decomposition parameter R_{21} plotted vs. period. The symbols are the same as in Figure 2.

at the Blazhko phase which corresponds to the largest amplitude.

Additional work is planned on these data, including seeing if one can determine phase shifts in maximum light as a function of wavelength, which can provide a useful test of pulsation models. So far, the only comparisons to models that we have performed is to the one-zone model of Grieco & Antonello (1990), the numerical values of which were provided to us by Antonello (private communication). The predicted and observed amplitudes match rather well, including the V, LWP and SWP wavelength regions. The closest match is for the largest amplitude Blazhko phase.

5. Concluding Remarks

This review has summarized the characteristics that must be explained by any theory of the Blazhko effect. Our intent in conducting the observing campaigns described in §3 was to provide a body of observations which cover complete pulsation cycles at various Blazhko phases, in order to make more detailed comparisons to theory possible. Clearly there is a great deal of analysis still to be done on these data, but it is also clear that (as usual) more studies are needed. The importance of intense coordinated campaigns for the study of phenomenon like the Blazhko effect is evident.

References:

Blazhko, S. 1907, *Astr. Nachr.*, **175**, 325.

Borkowski, K. J. 1980, *Space Sci. Rev.*, **27**, 511.

Cousens, A. 1983, *M.N.R.A.S.*, **200**, 807.

Cox, A. N. 1992, (this conference).

Grieco, A. & Antonello, E. 1990, in *Confrontation between Stellar Pulsation and Evolution*, ed. C. Cacciari & G. Clementini, (San Francisco: A.S.P.), p. 101.

Moskalik, P. 1986, *Acta Astron.*, **36**, 333.

Pérez, M., Loomis, C., Eaton, N., & Bradley, R. 1991, *Report to the IUE Three-Agency Coordination Committee.*

Preston, G. W., Smak, J., & Paczyński, B. 1965, *Ap. J. Suppl.*, **12**, 98.

Romanov, Yu. S., Udovichenko, S. N., & Frolov, M. S. 1987, *Sov. Astron. Lett.*, **13**, 29.

Simon, N. R. & Lee, A. S. 1981, *Ap. J.*, **248**, 291.

Simon, N. R. & Teays, T. J. 1982, *Ap. J.*, **261**, 586.

Szeidl, B., 1988, in *Multimode Stellar Pulsations*, eds. G. Kovács, L. Szabados, B. Szeidl (Budapest: Konkoly Observatory), p. 45.

Walraven, Th. 1949, *B. A. N.*, **11**, 17.

od. The symbols

DISCUSSION

P.MOSKALIK: Is the scatter in ϕ_{21} vs. Period (Simon & Teays 1982) due to Blazhko effect?

T.TEAYS: No, the stars in Simon & Teays were carefully selected to be ones which did not show Blazhko effect.

S. SREENIVASAN: Could one not look for Zeeman splitting measurements of the magnetic field?

T. TEAYS: It is difficult, since one needs fairly high resolution, and RR Lyr stars are faint. A fall-back approach might be to compare the equivalent widths of lines which are magnetic proxies and those which are essentially unaffected by a magnetic field, as a function of phase.

G. MATHYS: About the magnetic field, one should be aware that what the Russian group measured through polarimetry in RR Lyr is the line-of-sight component of the field, which can only be detected if the field has a sufficient large-scale organization. If one determine the field from unpolarized line shape, what one gets is the field modulus, which is different. Still, it would be valuable to confirm the polarimetric detection. I believe that the magnitude limitation should not be taken seriously. Indeed, I have been measuring fields in 12th magnitude stars from spectra recorded in circular polarization at ESO. The only requirement is that the spectral lines should not be too broad.

T. TEAYS: I agree, and I urge observers to try and confirm the magnetic field measurements in RR Lyr as a function of pulsation and Blazhko phase, since a definite answer would go a long way towards determining the cause of the phenomenon.

E. ANTONELLO: I am amazed at the qualitative agreement between the model predictions and the observations in the far UV region. Since the one zone model takes into account simply the static model atmospheres, I think the shock effects, which are presumably larger in the UV region, are possible less strong than what is suspected.

T. TEAYS: It's true that the good agreement may be partly fortuitous. As I mentioned, I selected the best match to show today. Your one-zone model appears to be generally in agreement with observations from V to $\approx$1500 Å.

THE BLAZHKO EFFECT IN RR LYRAE

T. J. TEAYS* and J. T. BONNELL**
Computer Sciences Corporation

E. G. SCHMIDT
National Science Foundation

E. F. GUINAN
Villanova University

and

T. G. BARNES III
McDonald Observatory, University of Texas

Abstract. We have conducted an observing campaign to study the Blazhko effect in RR Lyrae, using ground-based photometry and spectroscopy, along with low-resolution ultraviolet spectra with the *International Ultraviolet Explorer* (IUE). Observations were taken which followed a complete pulsation cycle, at a variety of Blazhko phases. The IUE observing shifts also provided a detailed V light curve, from measurements with IUE's Fine Error Sensor (FES). These data are analyzed using Fourier decomposition techniques.

Key words: RR Lyr – Blazhko effect.

1. Introduction

The Blazhko effect is the long term modulation of the amplitude and shape of the light and velocity curves of some (15-35 %) RR Lyr stars. In addition, emission in the hydrogen lines is seen at some Blazhko phases, but not others. For more detailed discussions see Preston et al. (1965), Szeidl (1988), and Teays (1993). RR Lyr's Blazhko period is $\approx$41 days. It also exhibits a tertiary period of $\sim$4 years, which modulates the Blazhko variation.

2. The Observations

We conducted observing campaigns in the summers of 1990 and 1991 to study the Blazhko effect in RR Lyr. The star was monitored throughout two IUE shifts (16 hours) in order to cover a complete pulsation cycle ($\approx$14 hours). This was done at several Blazhko phases. In the present report we are concentrating on preliminary results of the light curves determined from IUE's FES. The FES counts were corrected to V magnitudes using the calibration of Pérez et al. (1991).

* Staff Member of the International Ultraviolet Explorer Observatory.
** Compton Gamma Ray Observatory Science Support Center.

W. Wamsteker et al. (eds.), Frontiers of Space and Ground-Based Astronomy, 597–598.

TABLE I

Fourier decomposition parameters from FES light curves of RR Lyr

Date	R_{21}	φ_{21}
1991 May 21	0.40	4.08
1990 Jul 30	0.45	3.81
1990 Jul 11	0.37	4.11
1990 Jul 3	0.40	4.44
1990 Jun 27	0.55	3.79
1990 Jun 19	0.45	3.75

3. Results

The FES light curves were analyzed using Simon's (Simon & Lee 1981) Fourier decomposition techniques, which fit the V light curve by a time series of the form:

$$V = A_0 + \sum_{n=1}^{8} A_n \cos(n\omega t + \varphi_n).$$

Two useful parameters defined by Simon & Lee, *viz.*, $\varphi_{21} \equiv \varphi_2 - 2\varphi_1$ and $R_{21} \equiv A_2/A_1$, can be compared to the same values for field RR Lyr stars that do not show the Blazhko effect (Simon & Teays 1982). During the course of its Blazhko cycle, RR Lyr spans the range of parameters seen for the non-Blazhko variables. Therefore, the variation in *shape* of the light curves of different non-Blazhko variables (of similar period), matches the variation in the individual Blazhko variable, RR Lyr, as it goes through its Blazhko cycle. Comparison of the *amplitude* of pulsation for non-Blazhko variables and Blazhko variables indicates that the amplitudes are most similar when the Blazhko variable is at its maximum amplitude (Szeidl 1988). Table I lists the preliminary values of φ_{21} and R_{21} that were determined for RR Lyr at various Blazhko phases.

References

Pérez, M. R., Loomis, C., Eaton, N., & Bradley, R. 1991, *Report to the IUE Three-Agency Coordination Committee*

Preston, G. W., Smak, J., & Paczyński, B. 1965, *ApJS*, **12**, 98

Simon, N. R., & Lee, A. S. 1981, *ApJ*, **248**, 291

Simon, N. R., & Teays T. J. 1982, *ApJ*, **261**, 586

Szeidl, B. 1988, in *Multimode Stellar Pulsations*, ed. G. Kovács, L. Szabados, & B. Szeidl (Budapest: Konkoly Observatory), 45

Teays, T. J. 1993, in *New Perspectives on Stellar Pulsation and Pulsating Variable Stars*, ed. J. Nemec & J. Matthews (Cambridge: Cambridge University Press), in press

REPORT DOCUMENTATION PAGE

Form Approved
OMB No. 0704-0188

1. AGENCY USE ONLY *(Leave blank)*	2. REPORT DATE	3. REPORT TYPE AND DATES COVERED
	March 1995	Contractor Report

4. TITLE AND SUBTITLE
"Cepheid Temperature"
"The Blazhko Effect"

5. FUNDING NUMBERS
Code 684.1
NAS5-31845
Task 5779

6. AUTHOR(S)
Principal Investigator: T. Teays

7. PERFORMING ORGANIZATION NAME(S) AND ADDRESS(ES)
Computer Sciences Corporation
4061 Powder Mill Road
Calverton, MD 20705

8. PERFORMING ORGANIZATION REPORT NUMBER
RHPU0456

9. SPONSORING/MONITORING AGENCY NAME(S) AND ADDRESS(ES)
NASA Aeronautics and Space Administration
Washington, D.C. 20546-0001

10. SPONSORING/MONITORING AGENCY REPORT NUMBER
CR-189433

11. SUPPLEMENTARY NOTES
Technical Monitor: D. West, Code 684.1

12a. DISTRIBUTION/AVAILABILITY STATEMENT
Unclassified-Unlimited
Subject Category: 89
Report available from the NASA Center for AeroSpace Information,
800 Elkridge Landing Road, Linthicum Heights, MD 21090; (301) 621-0390.

12b. DISTRIBUTION CODE

13. ABSTRACT *(Maximum 200 words)*

Two separate research projects were covered under this contract. The first project was to study the temperatures of Cepheid variable stars, while the second was a study of the Blazhko effect in RR Larae, both of them using IUE data. They will be reported on separately, in what follows.

14. SUBJECT TERMS
Cepheid, Blazhko, RR Lyrae stars, IUE

15. NUMBER OF PAGES
2 (plus appendicies)

16. PRICE CODE

17. SECURITY CLASSIFICATION OF REPORT	18. SECURITY CLASSIFICATION OF THIS PAGE	19. SECURITY CLASSIFICATION OF ABSTRACT	20. LIMITATION OF ABSTRACT
Unclassified	Unclassified	Unclassified	Unlimited